

Re-Os isotope geochemistry of komatiite-hosted Ni-Cu-PGE deposits in Finland



M. Moilanen^{a,*}, E. Hanski^a, J. Konnunaho^b, S.-H. Yang^a, T. Törmänen^b, C. Li^c, L.M. Zhou^c

^a Oulu Mining School, P.O. Box 3000, FI-90014 University of Oulu, Finland

^b Geological Survey of Finland, P.O. Box 77, FI-96101 Rovaniemi, Finland

^c Key Laboratory of Re-Os Isotope Geochemistry, Chinese Academy of Geological Sciences, Beijing 100037, China

ARTICLE INFO

Keywords:

Re-Os isotopes
Ni-Cu-PGE sulfide and chromite
Komatiite
Archean
Paleoproterozoic
Finland

ABSTRACT

We have studied the Re-Os isotope systematics of komatiite-related Ni-Cu-PGE sulfide deposits in Finland, including the Archean Ruossakero Ni-(Cu), Vaara Ni-(Cu-PGE), Tainiovaara Ni-(Cu-PGE) deposits and Ni-PGE sulfide mineralization related to a dunitic body at Tulppio, and the Paleoproterozoic Lomalampi PGE-(Ni-Cu) deposit. We analyzed chromite separates from both mineralized and non-mineralized komatiitic rocks, bulk-sulfide separates, and country-rock black schist from one deposit, and for comparison, chromite separates from non-mineralized Archean komatiitic rocks from the Kovero and Kuhmo greenstone belts.

We have observed open-system behavior of sulfides in three deposits, with their Re-Os isotope compositions indicating resetting at ca. 1.83–1.87 Ga by metamorphic events related to the Svecofennian orogeny. Most of the chromite separates, especially those with > 10 ppb Os, retain their primary isotope compositions with near-chondritic initial $^{187}\text{Os}/^{188}\text{Os}$ ratios, indicating that their Os was derived from a mantle source with a chondritic Re-Os isotope evolution. These include the Vaara deposit, which yielded a chromite Re-Os isochron age of 2719 ± 140 Ma and low initial γOs of -1.2 ± 0.02 , in spite of the evidence for the presence of mass-independent S isotope fractionation in this deposit, suggesting a low-Os, sulfur-bearing contaminant. In the case of the Lomalampi deposit, chromites yield an isochron with an age of 2058 ± 93 Ma and initial γOs of $+0.9 \pm 0.02$, consistent with earlier isotope data from Central Lapland komatiites. However, one chromite from a mineralized cumulate gave a $\gamma\text{Os}(2050\text{ Ma})$ value of $+24 \pm 18$, indicating a minor/moderate degree of crustal contamination involving material from country rock black schists. This is also supported by earlier S isotope data. In the Archean Tainiovaara deposit, chromite also suggests crustal contamination ($\gamma\text{Os} + 13 \pm 1$), but country rocks are Os-poor Archean gneisses, leaving the source of radiogenic Os unclear, though it is possible that contamination occurred at a greater depth. Our results also provide evidence that the Re-Os age of the Ruossakero deposit is ca. 2.9 Ga, with the deposit likely representing komatiitic magmatism that is older than the komatiitic magmatism elsewhere in Finland. Re-Os results also confirmed that the mineralized Tulppio Dunite is Archean in age.

1. Introduction

Mafic and ultramafic rocks are important host rocks for magmatic Ni-Cu-Co-PGE sulfide deposits. In Finland, the past mining of Ni-Cu-(Co) sulfide ore has mainly been confined to the deposits related to the 1.88 Ga Svecofennian orogenic magmatism (Haapala and Papunen, 2015). So far, only one komatiite-related sulfide deposit, Tainiovaara in eastern Finland, has been mined in a small-scale operation in the late 1980's, although several small komatiite-hosted Ni-Cu-PGE sulfide deposits are known to occur in both Archean and Paleoproterozoic greenstone belts in the eastern and northern parts of the country

(Konnunaho, 2016). In addition, in the Central Lapland greenstone belt, the disseminated Ni-Cu-PGE sulfide deposit hosted by the ~2.06 Ga Kevitsa mafic-ultramafic intrusion is presently mined. The parental magma of the Kevitsa intrusion is suggested to be picritic to basaltic (Luolavirta et al., 2017). Another deposit close to Kevitsa, the Sakatti Cu-Ni-PGE sulfide deposit, which is related picritic or komatiitic magmatism (Brownscombe et al., 2015; Makkonen et al., 2017), has a great potential to become economically viable.

Experimental work and empirical observations have shown that magmatic sulfide deposits are the products of segregation of an immiscible sulfide-rich liquid from a silicate melt (e.g., Naldrett, 2004,

* Corresponding author.

E-mail address: marko.moilanen@oulu.fi (M. Moilanen).

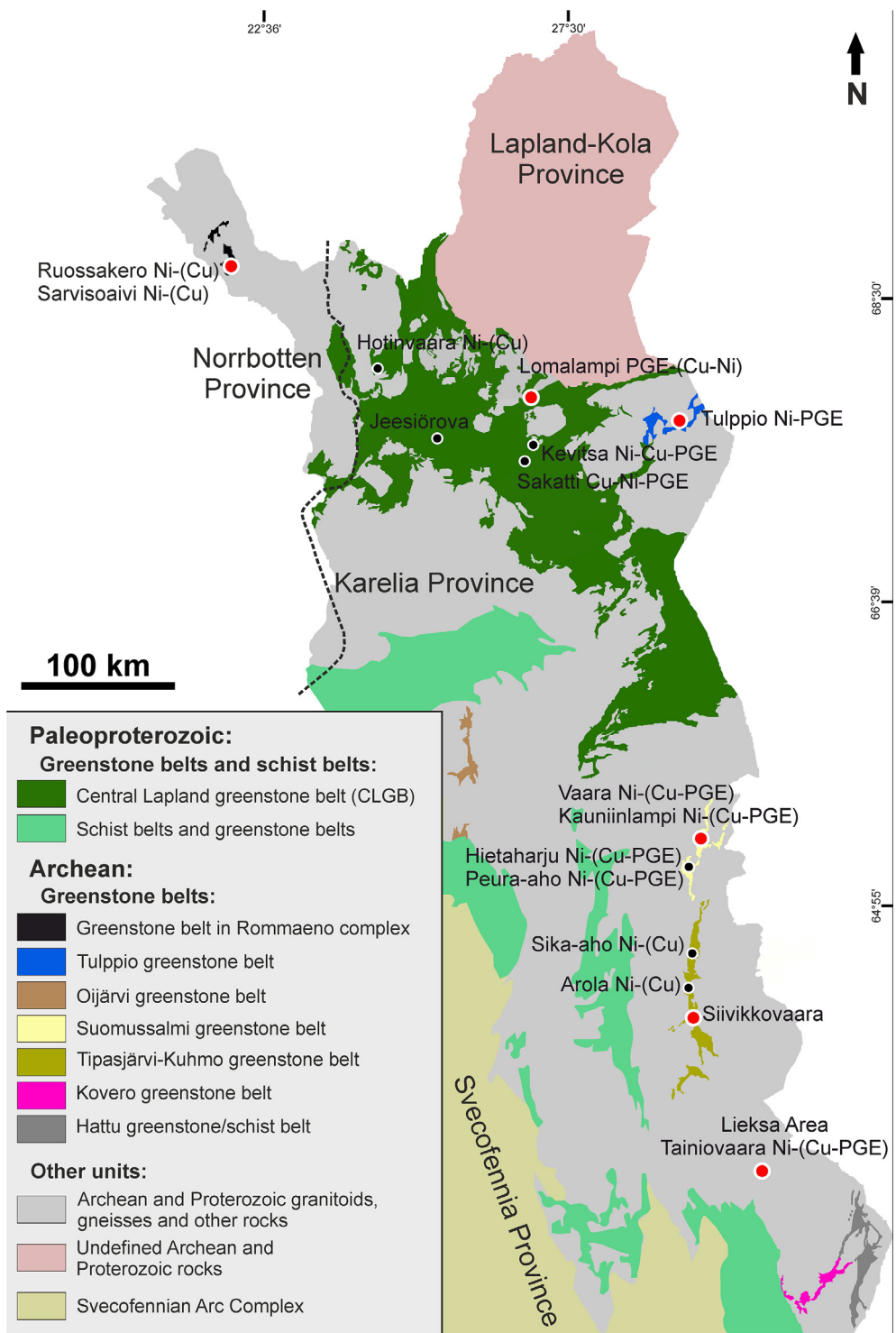


Fig. 1. Simplified geological map of Archean and Paleoproterozoic greenstone belts (GB) and schist belts in northern and eastern Finland, and locations of komatiite-hosted Ni-Cu-PGE deposits, Kevitsa Ni-Cu-PGE deposit and Sakatti Cu-Ni-PGE deposit. Dashed line indicates the boundary between the Karelia and Norrbotten Provinces. Modified after DigiKp (2018), Konnunaho et al. (2015), Konnunaho (2016) and Luukas et al. (2017).

and references therein). The sulfide liquid sequesters chalcophile metals from their parental silicate melt, which may lead to the formation of an economically viable magmatic Ni-Cu-Co-PGE deposits. Mantle-derived primitive melts, such as komatiitic or picritic magmas, are normally highly sulfur undersaturated when they are emplaced as lava flows or shallow-level intrusions (Mavrogenes and O'Neill, 1999; Smythe et al., 2017). Because of this, they normally need external sulfur to reach sulfide saturation (e.g., Mavrogenes and O'Neill, 1999; Lightfoot and

Keays, 2005; Keays and Lightfoot, 2010). Recent multiple sulfur isotope studies of komatiite-hosted Ni-Cu-PGE sulfide deposits have shown that contamination by S-bearing country rocks plays an important role in the genesis of these deposits (Bekker et al., 2009; Fiorentini et al., 2012; Konnunaho et al., 2013). However, Seat et al. (2009) showed, based on S isotope data from the Nebo-Babel deposit, that mantle-derived sulfur alone can be adequate to form a Ni-Cu sulfide deposit in some cases. Also, the study of sulfide saturation in mafic and ultramafic magmas by

Ripley and Li (2013) showed that formation of a Ni-Cu-PGE deposit via contamination or magma mixing but without addition of external S can be achieved in large-volume open systems (e.g., conduits, large-volume flood basalts) where the sulfide collection process is highly efficient.

The Re-Os isotope system provides a powerful tool for dating intrusive bodies and unravelling the origin of the magmas and related metal enrichment. Both Re and Os are chalcophile elements providing useful information on the ore-forming processes in magmatic Ni-Cu-PGE sulfide systems, including the role of crustal contamination (Lambert et al., 1998, 1999, 2000; Walker et al., 1994, 1997). Rhenium and Os are concentrated in the sulfide liquid, providing a good opportunity to study Re-Os isotopes in bulk sulfide samples or sulfide separates.

Based on the Re-Os isotope study of the Archean Kambalda Ni-Cu deposit in Western Australia, Foster et al. (1996) concluded that the komatiitic magma did not assimilate radiogenic crustal material during its turbulent flow/ascent or during magmatic processes before eruption. Their study also indicated that assimilation of sulfidic sedimentary rocks by thermal erosion by a komatiitic lava flow may not be an important factor in the ore genesis. Lambert et al. (1998) modelled the Kambalda Re-Os data published by Foster et al. (1996) and concluded that the Kambalda sulfide deposit was not formed by wholesale assimilation of country rock sedimentary rocks, though crustal contamination of komatiitic lava flows cannot be entirely ruled out, if the contaminant has a non-radiogenic Os isotope composition and low Re and Os concentrations, and the R factor was high (> 2000). In contrast, according to Lesher and Burnham (2001), sediment melting and assimilation by komatiitic magma was an important factor in the generation of the Kambalda Ni-Cu deposits and the S isotope composition of Kambalda sulfides is a more sensitive indicator of contamination than the Re-Os isotope systematics. The recent studies by Staude et al. (2016, 2017) have provided more evidence that the Ni ores at Kambalda were formed by thermomechanical erosion processes. Lahaye et al. (2001) measured Re-Os isotope compositions of 2.7 Ga komatiitic lava flows and related Ni-Cu sulfide deposits at Alexo, Texmont and Hart in the Abitibi greenstone belt, Canada. They concluded that the Alexo flow was contaminated with crustal material and in the Alexo and Hart flows, remobilization of Re and Os in sulfides by hydrothermal fluids occurred during the Grenville orogeny at ca. 1.2 Ga. On the other hand, the Texmont lava flow was not affected by this kind of localized hydrothermal alteration. Their study suggested that sulfide saturation was caused by assimilation of sulfide-bearing sedimentary rock. A later study on the Alexo lava flow by Gangopadhyay and Walker (2003) showed magmatic behavior of Re and Os in non-mineralized whole-rock samples.

In Finland, Re-Os isotope studies have been conducted on some layered intrusions and associated ore deposits, including Kevitsa (Hanski et al., 1997), Koitelainen and Akanvaara (Hanski et al., 2001a), and Kemi (Yang et al., 2016), but no systematic Os isotope studies of Finnish komatiite-hosted Ni-Cu-PGE deposits have so far been published. In this study, we apply the Re-Os isotope system to four Archean and one Paleoproterozoic komatiite-hosted sulfide deposits (Fig. 1). We have studied both mineralized and non-mineralized rocks from each location. Reference samples of non-mineralized komatiitic rocks were also collected from two greenstone belts. All the studied deposits and their host rocks have been affected by metamorphic processes to varying degrees, with chromite being the only partially preserved primary magmatic mineral phase. Because chrome spinel is generally resistant to secondary alteration processes and has a high Os content and low Re/Os ratio, it provides an excellent tool for obtaining information on the initial Os isotope composition of the related magmas (e.g., Walker et al., 1997; Gangopadhyay and Walker, 2003; Puchtel et al., 2001, 2007).

2. Geological background

2.1. Komatiitic magmatism in Finland and associated Ni-Cu-PGE deposits

Komatiitic-(± picritic) magmatism in Finland has occurred in several episodes in the Archean Era between ca. 2.95 and 2.75 Ga (Huhma et al., 2012a; Lehtonen et al., 2016) and in two major episodes, at ca. 2.5–2.4 Ga and 2.06–2.05 Ga, in the Paleoproterozoic Era (Hanski, 2012). Komatiites and associated mafic volcanic rocks are a typical component in Archean greenstone belts in eastern and northern Finland (e.g., Papunen et al., 2009; Maier et al., 2013; Makkonen et al., 2017), occasionally showing well-preserved spinifex textures (Hanski, 1980; Konnunaho et al., 2013). In most cases, they are chemically similar to the Munro-type komatiites (i.e., Al-unpleted) with no signs of interaction with ancient continental crust (Gruau et al., 1992; Huhma et al., 2012b; Konnunaho, 2016). However, they are strongly metamorphosed and have lost part of their original isotopic and geochemical signatures (Gruau et al., 1992).

The ca. ~2.4–2.5 Ga komatiites and komatiitic basalts, which are found in the Central Lapland greenstone belt, northern Finland, belong to the oldest volcanic rocks of the Paleoproterozoic Karelian formations deposited on the Archean basement and, in contrast to the Archean komatiites, are characterized by a very strong crustal signature manifested by relatively high silica contents, high LREE/HREE ratios and negative initial ϵ_{Nd} values (e.g., Räsänen et al., 1989; Hanski and Huhma, 2005; Hanski, 2012).

All the known ~2.05 Ga komatiitic rocks also occur in the Central Lapland greenstone belt (Hanski and Huhma, 2005), from where they continue to northern Norway (Barnes and Often, 1990). They are part of the Savukoski Group and, unlike typical komatiitic volcanic rocks worldwide, they often show volcaniclastic structures. Chemically, they are unique in being relatively high in TiO_2 and having hump-shaped chondrite-normalized REE patterns (Hanski et al., 2001b; Törmänen et al., 2016). They are spatially associated and genetically related to still more titaniferous, LREE-enriched picritic volcanic rocks, sharing a similarly positive initial ϵ_{Nd} (+4) demonstrating a long-term depletion in LREE in their mantle source (Hanski et al., 2001b; Gangopadhyay et al., 2006; Hanski and Kamenetsky, 2013). In contrast to the ~2.4–2.5 Ga komatiites, Nd isotope compositions indicate no or only minor crustal contamination (Hanski et al., 2001b).

Komatiite-hosted Ni-Cu-PGE deposits are found in both Archean and Paleoproterozoic greenstone belts in Finland (Fig. 1, Table 1). Recent reviews of these deposits can be found in Konnunaho et al. (2015), Konnunaho (2016), and Makkonen et al. (2017). The mineralization potential of komatiitic rocks in Finland has been studied by Maier et al. (2013), Heggie et al. (2013), Konnunaho et al. (2015), Konnunaho (2016), and Makkonen et al. (2017). In this study, we focus on three Archean deposits, Ruossakero in the Enontekiö-Käsivarsi area in the northwestern corner of Finnish Lapland, Vaara in the Suomussalmi greenstone belt in eastern Finland (Konnunaho et al., 2013; Konnunaho et al., 2015; Konnunaho, 2016), and Tainiovaara located in a small greenstone belt relict in eastern Finland (Konnunaho et al., 2015; Konnunaho, 2016). In addition, we studied one Archean dunitic body and related weak Ni-(PGE) mineralization at Tulppio in eastern Lapland (Heikura et al., 2010; Maier et al., 2013) and comparative samples of non-mineralized Archean komatiites from the Kovero greenstone belt (Konnunaho, 1999) and Kuhmo greenstone belt (Hanski, 1980; Papunen et al., 2009), both in eastern Finland. Paleoproterozoic deposits are represented by the ~2.05 Ga Lomalampi deposit (Törmänen et al., 2016) in the Central Lapland greenstone belt. Fig. 1 shows the research targets in different greenstone belts and Table 1 summarizes relevant information of the studied deposits.

2.2. The Archean Rommaeno complex and the Ruossakero Ni-(Cu) deposit

The Archean Ruossakero Ni-(Cu) sulfide deposit is located in the

Table 1
Summary of information on the studied deposits. Data from this study, Heikura et al. (2010), Konnunaho et al. (2015) and Törmänen et al. (2016). n.a. = not analyzed.

Deposit name	Area	Age	Parental magma	Deposit/mineralization type	Ni/Cu	Al ₂ O ₃ /TiO ₂	Pt/Pd	Pd/Ir	Ni tenor in 100% S
Ruossakero Ni-Cu Vaara Ni-(Cu-PGE)	Rommaeno complex Suomussalmi greenstone belt	Archean	Ti-depleted komatiite Al-undepleted komatiite	Disseminated, type I: Ni-Cu) Disseminated, type II: Ni-(Cu-PGE)	55–120	46	0.4	15	~23%
Tainiovaara Ni-(Cu-PGE)	Lieksta complex	Archean	Al-undepleted komatiite	Disseminated, type II and minor massive/semi massive, type I: Ni-(Cu-PGE)	13	19	0.4	28	~18–38%
Tulppio and related Ni-PGE mineralization Lomalampi PGE-(Ni-Cu)	Tulppio greenstone belt Central Lapland greenstone belt	Archean Paleoproterozoic	Al-undepleted, low Mg, Al-undepleted, low Mg, komatiite	Short intervals of weakly disseminated sulfides Disseminated low-grade, type II: PGE-(Ni-Cu)	19	23	0.4	10	~17–20%
					~12	30	0.8	n.a.	~125%
					4	15	2	15	~6–9%

central part of the Archean Rommaeno Complex in the northwestern corner of Finnish Lapland (Fig. 1). The mineralized ultramafic bodies are associated with supracrustal rocks of the Ropi Suite comprising three lithodemes: i) Sarvisoaini, ii) Tarju, and iii) Pailujärvi (DigiKP, 2018; Karinen et al., 2015). The Archean rocks are locally covered by Paleoproterozoic supracrustal rocks. The lowermost Archean unit (Sarvisoaini lithodeme) comprises mafic to ultramafic volcanic rocks (i.e., komatiitic olivine-(± pyroxene) cumulate and non-cumulate rocks) and mafic volcanic rocks, minor sulfide-bearing felsic volcanic rocks, and BIF interlayers (Konnunaho et al., 2015; Karinen et al., 2015). Felsic volcanic rocks have yielded a U-Pb zircon age of ca. 2.93 Ga (Karinne et al., 2015). The Ruossakero area is dominated by komatiitic cumulate rocks, including homogeneous, massive, and medium- to coarse-grained metamorphosed peridotites and dunites as well as minor pyroxenites in association with dunites. The rocks were metamorphosed under amphibolite facies conditions, and the primary silicates have been replaced mainly by serpentine as well as chlorite, amphibole, talc, and carbonate (Fig. 2c). They commonly contain olivine and pyroxene of metamorphic origin. Despite the pervasive alteration, primary cumulus textures can still be recognized locally in ultramafic cumulates. The komatiites that represent non-cumulates contain variable proportions of amphibole (tremolite), chlorite, serpentine, talc and metamorphic olivine (Konnunaho et al., 2015).

The Ruossakero komatiitic body is one of the largest ultramafic lenses in the Rommaeno Complex (Konnunaho et al., 2015). On the surface, the lens is ~7 km in length and from 500 m to 3 km in width. It can be divided into two parts, the Main body and the Small body. Disseminated Fe-Ni-Cu sulfides (Fig. 2h) have been found in several distinct subzones in both bodies, occurring in Cr-poor komatiitic olivine cumulates (meso- and adcumulates). The mineralization at Ruossakero belongs to the type II of Lesher and Keays (2002) and the PGE-poor Ni-(Cu) deposit subtype (Konnunaho, 2016). The sulfide assemblage is dominated by pyrite and millerite (± violarite) with occasional chalcopyrite, pentlandite and pyrrhotite, indicating post-magmatic low-temperature hydrothermal oxidation of the primary magmatic pyrrhotite-pentlandite-chalcopyrite assemblage (Konnunaho et al., 2015). The main oxide phases are partially altered chromite, Cr-magnetite and magnetite (Fig. 3c).

2.3. The Archean Tulppio greenstone belt and the Tulppio Ni-PGE mineralization

The Tulppio Dunite occurs in the Tulppio greenstone belt in eastern Lapland, which is part of the larger Archean Tuntsa Terrain (Juopperi and Vaasjoki, 2001; Sorjonen-Ward and Luukkonen, 2005). The belt is composed of felsic to ultramafic (komatiitic) volcanic rocks and associated mica schists and gneisses. The Tulppio Dunite is 1.5 × 4.5 km in size and comprises medium-grained olivine cumulates with some peridotitic to gabbroic cumulates at the contacts. Olivine is well preserved (Fig. 2f) in the central part of the body and becomes more altered towards the contacts. Based on the maximum Fo content of olivine (~91 mol%), the ultramafic body had a low-Mg komatiitic parental magma.

The Geological Survey of Finland (GTK) conducted exploration work in the area between 2005 and 2008, including a diamond drillhole profile across the middle part of the dunite body. Two successive drillholes intersected a horizon of weak sulfide mineralization (0.15–0.46 wt% S) with up to 1.53 and 0.81 ppm of combined Pt + Pd, slightly elevated Ni (0.1–0.3 wt% sulfidic Ni) and traces of Cu (≤ 0.011 wt%) over a 1.5 m interval. Two holes drilled on both sides of the main profile encountered broader zones of weakly PGE-mineralized dunite, e.g., 5 m with 0.14–0.27 ppm of Pt + Pd and several 1.5-m-thick intersections with 0.1–0.26 ppm (Heikura et al., 2010). The low-grade intersections (< 0.5 ppm Pt + Pd) show low Pt/Pd ratios of 0.3–0.8, whereas the higher-grade intersections tend to have higher relative Pt contents, with Pt/Pd falling in the range of 0.8–1.5. The sulfide

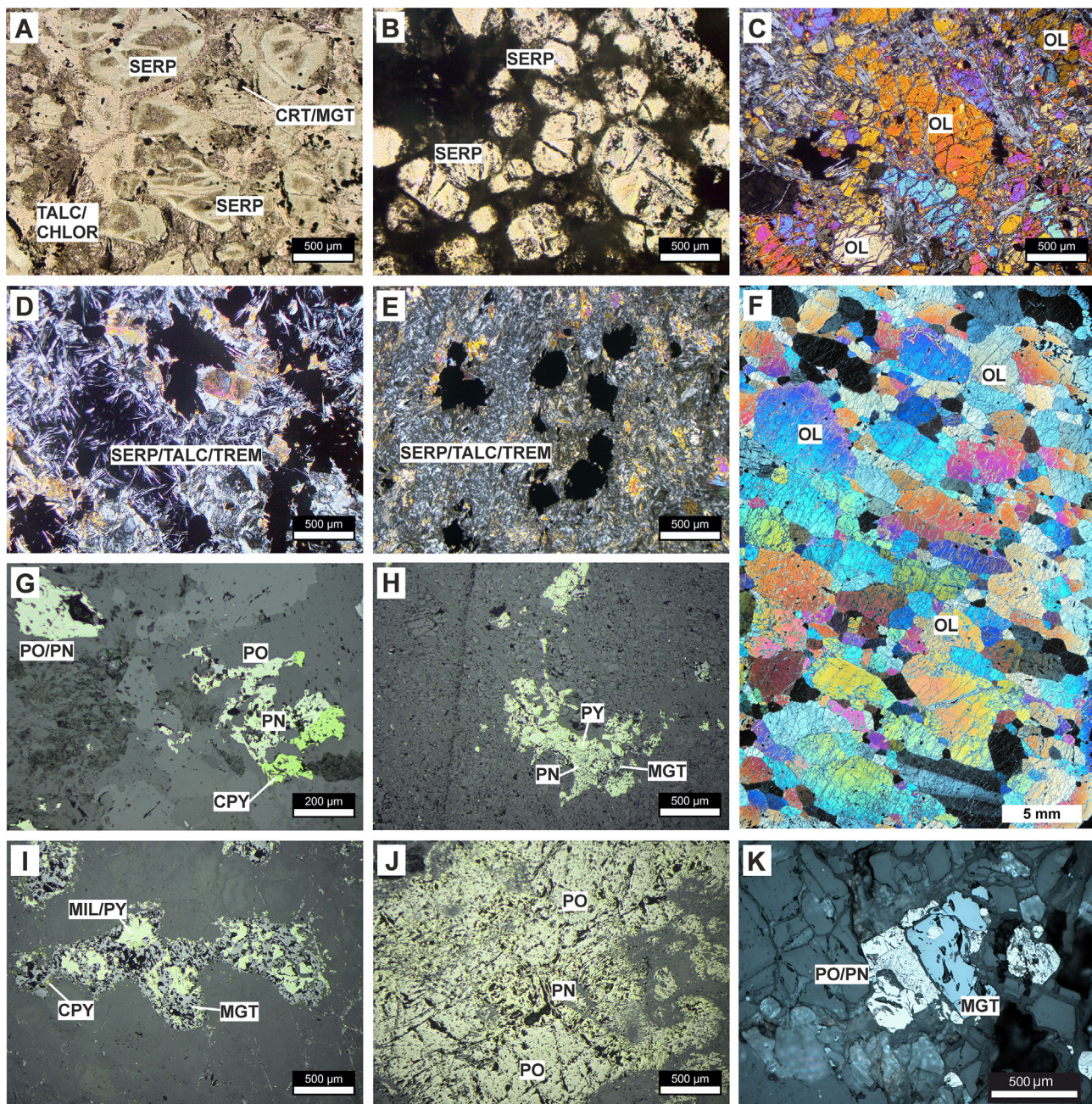


Fig. 2. Photomicrographs of different rock types and sulfide minerals. A) Serpentinized olivine cumulate from the Lomalampi deposit; B) Serpentinized olivine cumulate from the Vaara deposit; C) Well-preserved dunite from the Ruossakero deposit; D) Highly altered olivine cumulate from the Tainiovaara deposit; E) Highly altered olivine cumulate from the Kovero area; F) Well-preserved dunite from the Tulppio ultramafic body; G) Disseminated sulfides from the Lomalampi deposit; H) Disseminated sulfides and oxides from the Ruossakero deposit; I) Interstitial sulfide blebs partly replaced by magnetite in the Vaara deposit; J) Semi-massive sulfides from the Tainiovaara deposit; K) Sulfides from the Tulppio mineralization. A-B taken in transmitted, plane-polarized light, and C-F in transmitted, cross-polarized light and G-K in reflected light. Abbreviations: CHLOR = chlorite, CPY = chalcopyrite, CRT = chromite, MGT = magnetite, MIL = millerite, OL = olivine, PN = pentlandite, PO = pyrrhotite, PY = pyrite, SERP = serpentinite, TREM = tremolite.

paragenesis containing pyrrhotite and pentlandite is typical for komatiite-hosted Ni mineralization (Fig. 2k). The oxides are mainly composed of chromite and magnetite (Fig. 3b).

2.4. The Archean Suomussalmi greenstone belt and the Vaara Ni-(Cu-PGE) deposit

The Archean Suomussalmi greenstone belt represents the northernmost segment of the Tipasjärvi-Kuhmo-Suomussalmi greenstone belt complex in eastern Finland (Papunen et al., 2009) (Fig. 1). According to Papunen et al. (2009), the Suomussalmi greenstone belt consists of five

lithostratigraphic formations being, from oldest to youngest: 1) Luoma, 2) Mesa-aho, 3) Tervonen, 4) Saarikylä, and 5) Huutoniemi. Komatiitic rocks including the host-rocks of the Vaara deposit are part of the Saarikylä Formation. The immediate footwall of the Vaara ultramafic body are phyllites, black schists and sulfide-bearing sericite schists, belonging to the Mesa-aho Formation. Further to the west, felsic volcanic rocks of the Luoma Formation occur. Due to folding, there are also felsic volcanic rocks intervening with cumulate rocks in the Vaara area, and these could also be part of the Saarikylä Formation. The phyllite-black schist association to the east and the tholeiitic basalts on the southern and northern flanks of the Vaara body are assigned to the

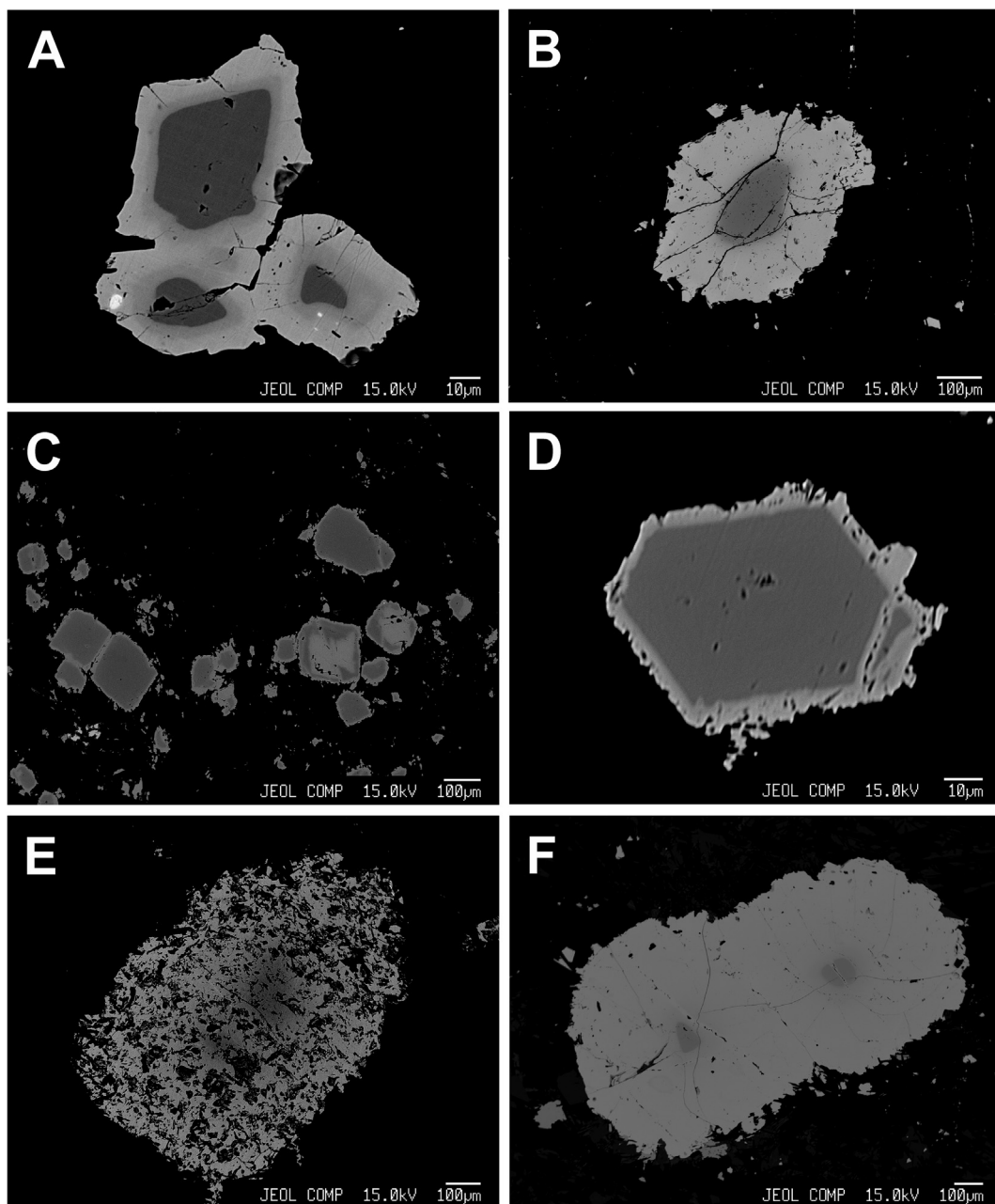


Fig. 3. Back-scattered electron images of chromite grains in the studied komatiite-hosted sulfide deposits, showing variable degrees of alteration. A) Subhedral chromite grains from the Lomalampi PGE-(Ni-Cu) deposit. Note the base metal sulfide inclusions. B) Anhedral, altered chromite grain from the Tulppio Ni-PGE mineralization. C) Anhedral and subhedral chromite grains from the Ruossakero Ni-(Cu) deposit. D) Well-preserved euhedral chromite grain from the Vaara Ni-(Cu-PGE) deposit. E) Highly altered, subhedral chromite grain from the Tainiovaara Ni-(Cu-PGE) deposit. F) Highly altered, subhedral chromite grains in unmineralized komatiite from the Kovero area.

Huutoniemi and Tervonen Formations, respectively (Papunen et al., 2009).

The komatiitic extrusive body at Vaara is one of five ultramafic lenses forming a 15-km-long, N-S-trending chain of ultramafic bodies in the Saarikylä area. On the surface, the Vaara ultramafic lens is approximately 1 km long and 400 m wide (Konnunaho et al., 2013; Konnunaho et al., 2015). The sulfide deposit is composed of disseminated sulfides in the central part of Cr-poor olivine mesocumulates (Fig. 2b). It belongs to the type II (Lesher and Keays, 2002) and PGE-enriched Ni-(Cu-PGE) deposit subtypes. The deposit consists of 3 separate mineralized horizons with thicknesses from ~2–3 m to ~50 m. The sulfides are dominated by the pyrite–millerite–violarite assemblage while pentlandite and chalcopyrite are less abundant, though

locally important (Fig. 2i). A small amount of well-preserved chromite occurs in the deposit (Fig. 3d). Extensive replacement of interstitial sulfides by magnetite (Fig. 2i) and the presence of pyrite and Ni-rich sulfides without pyrrhotite indicate post-magmatic, low-temperature hydrothermal oxidation of the primary magmatic pyrrhotite–pentlandite–chalcopyrite assemblage and significant concomitant loss of sulfur (Konnunaho et al., 2013). This process led to substantial upgrading of the original metal tenors of the deposit (Table 1).

2.5. The Archean Lieksa complex and the Tainiovaara Ni-(Cu-PGE) deposit

Small ultramafic bodies and associated amphibolites are found as greenstone belt relicts surrounded by tonalite gneisses in the Archean

Table 2

Sample descriptions. Abbreviations: (D) = duplicate sample. Minerals: amph = amphibole, chl = chlorite, cpy = chalcopyrite, crb = carbonate, crt = chromite, ilm = ilmenite, mgt = magnetite, mil = millerite, ol = olivine, pn = pentlandite, po = pyrrhotite, py = pyrite, trem = tremolite, trem = serpentine, trem = violarite. Peak metamorphic facies information from Metamorphism of Finland 1:100 000 digital dataset, 2018.

Deposit/area	Sample id	Drillhole, sampling interval	Rock type	Metamorphic facies	Description	Mineralization type	Mineral separate
Lomalampi PGE-(Ni-Cu)	LOM-1	R407 52.50-55.50	Olivine cumulate/ peridotite	Low-middle amphibolite facies	Mineralized altered olivine cumulate (peridotite). Major minerals: serp, talc and chl. Cumulus texture is preserved. Oxides: mgt, altered crt, ilm. Contains disseminated sulfides.	Mineralized: disseminated sulfides (pn, po, cpy)	Oxide
Lomalampi PGE-(Ni-Cu)	LOM-2(D)	R407 61.25-64.25	Olivine cumulate/ peridotite	Low-middle amphibolite facies	Mineralized altered olivine cumulate (peridotite). Major minerals: serp, talc and chl. Cumulus texture is preserved. Oxides: mgt, altered crt. Sulfides as dissemination and veins.	Mineralized: disseminated sulfides (pn, po, cpy)	Oxide
Lomalampi PGE-(Ni-Cu)	LOM-3	R407 41.00-43.20	Olivine cumulate/ peridotite	Low-middle amphibolite facies	Mineralized altered olivine cumulate (peridotite). Major minerals: serp, amph, talc, chl. Cumulus texture is preserved. Oxides: mgt, altered crt. Disseminated sulfides.	Mineralized: disseminated sulfides (pn, po, cpy)	Oxide
Lomalampi PGE-(Ni-Cu)	LOM-4	R406 8.00-11.00	Olivine cumulate/ peridotite	Low-middle amphibolite facies	Mineralized altered olivine cumulate (peridotite). Major minerals: serp, amph, talc, chl. Cumulus texture is preserved. Oxides: mgt, altered crt. Disseminated sulfides.	Mineralized: disseminated sulfides (po, pn, cpy)	Oxide
Lomalampi PGE-(Ni-Cu)	LOM-5	R403 74.00-76.55	Olivine cumulate/ peridotite	Low-middle amphibolite facies	Altered olivine cumulate (peridotite). Major minerals: serp (visible olivine pseudomorphs), amph, chl. Oxides: mgt, altered crt, ilm.	Non-mineralized	Oxide
Lomalampi PGE-(Ni-Cu)	LOM-6	R409 50.00-52.80	Olivine cumulate/ peridotite	Low-middle amphibolite facies	Altered olivine cumulate (peridotite). Major minerals: amph, talc, chl. Oxides: mgt and altered crt. Cumulus texture is somewhat preserved.	Non-mineralized	Oxide
Lomalampi PGE-(Ni-Cu)	LOM-7	R410 44.15-48.05	Olivine cumulate/ peridotite	Low-middle amphibolite facies	Highly altered olivine cumulate (peridotite). Major minerals: amph, talc, chl. Oxides: mgt, altered crt, ilm.	Non-mineralized	Oxide
Lomalampi PGE-(Ni-Cu)	LOM-1_S	R407 61.25-64.25	Olivine cumulate/ peridotite	Low-middle amphibolite facies	Mineralized altered olivine cumulate (peridotite). Major minerals: serp, talc and chl. Cumulus texture is preserved. Oxides: mgt, altered crt. Some sulfides.	Disseminated sulfides (pn, po, cpy)	Sulfide
Lomalampi PGE-(Ni-Cu)	LOM-2_S	R407 52.50-55.50	Olivine cumulate/ peridotite	Low-middle amphibolite facies	Mineralized altered olivine cumulate (peridotite). Major minerals: serp, talc and chl. Cumulus texture is preserved. Oxides: mgt, altered crt. Some sulfides.	Disseminated sulfides (pn, po, cpy)	Sulfide
Lomalampi PGE-(Ni-Cu)	LOM-3_WR	R406 56.35-59.65_A	Black schist	Low-middle amphibolite facies	Foliated highly deformed black schist. Major minerals: biotite, quartz and graphite.	Graphite-rich black schists. No visual sulfides	Whole-rock
Lomalampi PGE-(Ni-Cu)	LOM-5_WR	R406 56.35-59.65_B	Black schist	Low-middle amphibolite facies	Foliated highly deformed black schist. Major minerals: biotite, quartz and graphite. Contains sulfide-crb veins.	Sulfides (py, po, cpy) with sheared and disseminated texture	Whole-rock
Lomalampi PGE-(Ni-Cu)	LOM-4_WR	R439 76.20-76.30	Black schist	Low-middle amphibolite facies	Foliated highly deformed black schist. Major minerals: biotite, quartz and graphite. Contains sulfides.	Spotted pyrite and disseminated sulfides (py, po, cpy)	Whole-rock
Vaara Ni-(Cu-PGE)	VAA-1	R631 77.15-79.30	Olivine cumulate	Middle amphibolite facies	Altered olivine cumulate. Major minerals: sep, talc. Oxides: altered crt and mgt.	Non-mineralized	Oxide
Vaara Ni-(Cu-PGE)	VAA-2	R631 103.95-106.95	Olivine cumulate	Middle amphibolite facies	Altered olivine cumulate. Major minerals: sep, talc. Oxides: altered crt and mgt	Non-mineralized	Oxide
Vaara Ni-(Cu-PGE)	VAA-3	R634 41.70-44.90	Olivine cumulate	Middle amphibolite facies	Altered olivine cumulate. Major minerals: sep, talc. Oxides: altered crt and mgt	Non-mineralized	Oxide
Vaara Ni-(Cu-PGE)	VAA-4	R636 50.00-53.00	Olivine cumulate	Middle amphibolite facies	Altered olivine cumulate. Major minerals: sep, talc, chl. Oxides: altered crt and mgt. Contains sulfides.	Mineralized: disseminated sulfides (py, pn, po, mil, vio, cpy)	Oxide
Vaara Ni-(Cu-PGE)	KOM-5	R635 28.80-31.10	Pyroxenite cumulate	Middle amphibolite facies	Altered pyroxenite cumulate. Major minerals: sep, chl, talc, amph. Oxides: altered crt and mgt	Non-mineralized	Oxide
Vaara Ni-(Cu-PGE)	KOM-6	R635 34.60-35.85	Pyroxenite cumulate	Middle amphibolite facies	Mineralized altered olivine cumulate. Major minerals: sep, talc, chl. Cumulus texture preserved. Oxides: altered crt and mgt. Contains disseminated sulfides.	Disseminated sulfides (py, pn, po, mil, vio, cpy)	Sulfide
Vaara Ni-(Cu-PGE)	VAA-1_S	R636 101.50-104.50	Olivine cumulate	Middle amphibolite facies	Mineralized altered olivine cumulate. Major minerals: sep, talc, chl. Oxides: altered crt and mgt. Contains disseminated sulfides.	Disseminated sulfides (py, pn, po, mil, vio, cpy)	Sulfide
Vaara Ni-(Cu-PGE)	VAA-2_S	R633 4.90-8.00	Olivine cumulate	Middle amphibolite facies	(continued on next page)		

Table 2 (continued)

Deposit/area	Sample id	Drillhole, sampling interval	Rock type	Metamorphic facies	Description	Mineralization type	Mineral separate
Tainiovaara Ni-(Cu-PGE)	TAI-1	R311 17.85-20.85	Olivine cumulate/serpentinite	High amphibolite facies	Altered olivine cumulate. Major minerals: amph, chl, serp, talc and some crb and trem. Oxides: altered crt and mgt	Non-mineralized	Oxide
Tainiovaara Ni-(Cu-PGE)	TAI-2	R303 53.25-56.25	Olivine cumulate/serpentinite	High amphibolite facies	Mineralized altered olivine cumulate. Major minerals: serp, talc, amph. Oxides: altered crt and mgt. Contains disseminated and sheared sulfides.	Mineralized (pn, po, trace cpv)	Oxide
Tainiovaara Ni-(Cu-PGE)	TAI-3_S	R304 92.50-95.50	Olivine cumulate/serpentinite	High amphibolite facies	Mineralized altered olivine cumulate. Major minerals: serp, talc, amph. Oxides: altered crt and mgt. Contains disseminated and sheared sulfides.	Mineralized (po, pn)	Sulfide
Tainiovaara Ni-(Cu-PGE)	TAI-1_S (D)	R307 47.40-50.40	Olivine cumulate/serpentinite	High amphibolite facies	Mineralized altered olivine cumulate. Major minerals: serp, talc, amph. Oxides: altered crt and mgt. Contains disseminated and sheared sulfides.	Mineralized (pn, po, trace cpv)	Sulfide
Tulppio Ni-PGE mineralization	TUL-1	R307 47.00-49.60	Dunite	Middle amphibolite facies	Highly altered and sheared dunite. Major minerals: serp, talc. Oxides: altered crt.	Non-mineralized	Oxide
Tulppio Ni-PGE mineralization	TUL-2	R314 73.90-76.90	Dunite	Middle amphibolite facies	Relatively fresh dunite. Major minerals: ol, serp. Oxides: altered crt.	Non-mineralized	Oxide
Tulppio Ni-PGE mineralization	TUL-3	R320 5.20-8.20	Dunite	Middle amphibolite facies	Relatively fresh dunite. Major minerals: ol, serp. Oxides: altered crt.	Non-mineralized	Oxide
Tulppio Ni-PGE mineralization	TUL-4	R320 98.40-101.40	Dunite	Middle amphibolite facies	Relatively fresh dunite. Major minerals: ol, serp. Oxides: altered crt.	Non-mineralized. Ni-PGE-enriched zone with disseminated sulfides in same drillhole (pn, po, and py) ~ 23 m above this sample	Oxide
Ruossakero Ni-(Cu)	RUO-1	R416 25.45-28.45	Serpentinite	Middle-high amphibolite facies	Highly altered olivine cumulate. Major minerals: serp, talc, crb. Oxides: Cr-ngrt.	Non-mineralized, remobilized Cr-ngrt veins (possibly been chromite in origin)	Oxide
Ruossakero Ni-(Cu)	RUO-2	R416 69.15-72.00	Serpentinite	Middle-high amphibolite facies	Highly altered olivine cumulate. Major minerals: serp, talc. Oxides: Cr-ngrt.	Non-mineralized, remobilized Cr-ngrt veins (possibly been chromite in origin)	Oxide
Ruossakero Ni-(Cu)	RUO-3 (D)	R417 102.00-105.00	Serpentinite	Middle-high amphibolite facies	Highly altered olivine cumulate. Major minerals: serp, talc. Oxides: mgt and altered crt.	Non-mineralized	Oxide
Ruossakero Ni-(Cu)	RUO-4	R434 101.65-104.65	Dunite/peridotite/olivine cumulate	Middle-high amphibolite facies	Mineralized altered dunite. Major minerals: ol, serp. Oxides: altered crt and mgt. Contains sulfides.	Mineralized: disseminated sulfides (py, mil, po)	Oxide
Ruossakero Ni-(Cu)	RUO-5	R413 171.20-174.20	Olivine cumulate/serpentinite	Middle-high amphibolite facies	Mineralized altered dunite. Major minerals: serp, chl. Oxides: altered crt and mgt. Contains sulfides.	Mineralized: disseminated sulfides (py, mil, po)	Oxide
Ruossakero Ni-(Cu)	RUO-2_S	R434 185.60-188.60	Dunite/olivine cumulate	Middle-high amphibolite facies	Mineralized altered dunite. Major minerals: ol, amph, serp. Oxides: altered crt and mgt. Contains sulfides.	Disseminated sulfides (py, mil, po)	Sulfide
Ruossakero Ni-(Cu)	RUO-1_S	R413 107.00-110.00	Dunite/olivine cumulate	Middle-high amphibolite facies	Mineralized altered dunite. Major minerals: ol, serp, chl. Oxides: altered crt and mgt. Contains sulfides.	Disseminated sulfides (py, mil, po)	Sulfide
Kovero	KOM-1	KOV-010 13.50-14.50	Komatite lava facies	Middle amphibolite facies	Highly altered serpentinite. Main minerals: trem, amph, serp, chl, talc, crb. Oxides: highly altered crt and mgt.	Non-mineralized	Oxide
Kovero	KOM-2 (D)	KOV-010 14.50-15.70	Komatite lava facies	Middle amphibolite facies	Highly altered serpentinite. Main minerals: trem, amph, serp, chl, talc, crb. Oxides: highly altered crt and mgt.	Non-mineralized	Oxide
Kovero	KOM-3	KOV-02 7.00-8.50	Komatite lava facies	Middle amphibolite facies	Highly altered serpentinite. Main minerals: trem, amph, serp, chl, talc, crb. Oxides: highly altered crt and mgt.	Non-mineralized	Oxide
Kovero	KOM-4	KOV-02 12.90-13.80	Komatite lava facies	Middle amphibolite facies	Highly altered serpentinite. Main minerals: trem, talc, crb. Oxides: highly altered crt and mgt.	Non-mineralized	Oxide
Sivikkovaara	KOM-8	SII-005 83.00-85.80	Komatite lava facies	Middle amphibolite facies	Altered serpentinite. Main minerals: trem, chl. Oxides: altered crt and mgt.	Non-mineralized	Oxide

Lieksa complex, eastern Finland (Halkoaho and Niskanen, 2004) (Fig. 1). One of the ultramafic bodies occurs at Tainiovaara, forming an approximately 180-m-long and 80-m-wide, intensively deformed and metamorphosed olivine mesocumulate lens. It hosts a small Ni-(Cu-PGE) deposit (Pekkarinen, 1980; Vanne, 1981; Konnunaho et al., 2015), which was partly mined in 1989.

The Tainiovaara Ni-(Cu-PGE) deposit consists mainly of disseminated sulfides (type II; Lesher and Keays, 2002) (Fig. 2d and 2j), but there are also small massive to semi-massive and net-textured sulfide accumulations (type I) at the bottom of the Cr-poor olivine mesocumulate lens (Vanne, 1981; Papunen, 1989; Konnunaho et al., 2015). The deposit is slightly enriched in Cu and PGE, but not as much as in some other Finnish PGE-enriched deposits (e.g., Lomalampi and Vaara) (Konnunaho et al., 2015; Konnunaho, 2016). The major ore minerals are pyrrhotite and pentlandite while chalcopyrite and pyrite are minor phases, thus representing only a slightly modified magmatic sulfide assemblage. The main oxide minerals are magnetite and chromite, with the latter being generally highly altered (Fig. 3e).

2.6. The Paleoproterozoic Central Lapland greenstone belt and the Lomalampi PGE-(Ni-Cu) deposit

The Lomalampi deposit is located in the central part of the Paleoproterozoic Central Lapland greenstone belt (CLGB) (Fig. 1). The CLGB extends approximately 400 km from the Russian border in the east to the Norwegian border in the north (Fig. 1). It was formed during prolonged stages of rifting of the Archean basement with deposition of Karelian sedimentary and volcanic rocks in intracratonic and cratonic margin rift settings between 2.5 Ga and 2.0 Ga (Lehtonen et al., 1998; Hanski and Huhma 2005). These rifting events were followed by multiple deformation and metamorphic events and associated minor felsic and mafic magmatism related to the Svecofennian orogenic events between 1.91 and 1.80 Ga. The youngest supracrustal rock sequences in the CLGB are represented by post-1.88 Ga molasse-type deposits (Lehtonen et al., 1998; Hanski and Huhma 2005). In this paper, we focus on komatiitic rocks belonging to the Savukoski Group, which contains the majority of the komatiitic rocks of the CLGB, including the komatiite-hosted Lomalampi PGE-(Ni-Cu) mineralization. The lower part of the Savukoski Group consists of fine-grained metasedimentary rocks, such as black schists and phyllites with subordinate amounts of graywackes, mafic tuffites and dolomites. These metasediments are overlain by komatiitic and picritic volcanic rocks and related basaltic differentiates.

The age of the Savukoski Group rocks is constrained by the U-Pb zircon age of 2058 ± 4 Ma measured for the cross-cutting Kevitsa Ni-Cu sulfide-bearing layered intrusion (Mutanen and Huhma, 2001). Komatiitic rocks in the Jeesiörova area (Fig. 1) have yielded a clinopyroxene-whole-rock Sm-Nd age of 2056 ± 25 Ma, which is the best currently available direct age determination for the komatiites of the Savukoski Group (Hanski et al., 2001b).

Komatiitic rocks in the Lomalampi area occur as volcanoclastic deposits, thin lava flows, and several olivine ± pyroxene cumulate bodies. The ultramafic rocks have been metamorphosed under greenschist to lower amphibolite facies conditions producing serpentinite-chlorite-talc ± amphibole assemblages (Törmänen et al., 2016). The host unit the Lomalampi PGE-(Ni-Cu) deposit is a sheet-like olivine orthocumulate body 30–65 m in thickness and ~700 m in length (Fig. 2a), representing either a sill or a cumulate part of a thick lava flow. The sulfide mineralization is formed by a zone of disseminated sulfides (type II) varying from a few meters to 40 m in thickness. The sulfide assemblage is composed of pyrrhotite with subordinate amounts of pentlandite and chalcopyrite and traces of sulfarsenides and diarsenides (Fig. 2g). The main oxide minerals are chromite (Fig. 3a) and magnetite. Compared to other Finnish komatiite-hosted Ni-Cu-PGE deposits, the Lomalampi deposit is low in Ni (generally 0.1–0.3 wt%) and Cu (0.05–0.1 wt%) but shows relatively high PGE concentrations

(up to 2 ppm) and an exceptionally high Pt/Pd ratio (2.2) for a komatiite-hosted sulfide deposit (commonly around 0.5) (Konnunaho et al., 2015; Törmänen et al., 2016).

3. Sampling and analytical methods

All samples were taken from drillcores and represent different types of mineralized and non-mineralized rock types (Table 2). The length of the sampled cores vary from about 1 to 3 m. We utilized a portable X-Ray Fluorescence (pXRF) analyzer for locating Cr-rich core intervals for chromite separation. Mineral separates were obtained using standard heavy liquids techniques. Purified chromite concentrates were ground in an agate mortar to avoid metal contamination. Whole-rock samples were crushed and powdered with an agate ring-mill. A total of 42 samples (30 chromite separates, 9 bulk sulfide samples and 3 whole-rock samples) were included in this study.

The isotopic compositions of Re and Os were determined at the Key Re-Os Laboratory of China, the Academy of Geological Sciences. Precisely weighed powders (~0.06 g for chromite and sulfide separates and ~0.23 g for whole-rock samples) were loaded into Carius tubes together with ^{185}Re and ^{190}Os spikes and digested by reverse aqua regia in the presence of a small amount of H_2O_2 (Shirey and Walker, 1998). The tube was heated in an oven at 230°C for about 24 h. Osmium was separated as OsO_4 by distillation at $105\text{--}110^\circ\text{C}$ and trapping by Milli-Q water. During distillation, the reverse aqua regia acted as an oxidizer. Rhenium was extracted from the residue by acetone in a 5 M NaOH solution. A more detailed description of the separation procedure is available in Du et al. (2001, 2004). Rhenium and Os concentrations and isotopic compositions were measured by a Thermo Fisher Scientific Triton-plus mass spectrometer operating in negative ion detection mode (Greaser et al., 1991) and equipped with an oxygen gas leak valve and an ion counting multiplier. The intensity of $^{192}\text{OsO}_3$ was used to monitor the interference of ^{187}Os with ^{187}Re , and the intensity of $^{185}\text{ReO}_3$ was used to monitor the interference of ^{187}Re on ^{187}Os . Instrumental mass fractionation of Os was corrected by normalizing the measured $^{192}\text{Os}/^{188}\text{Os}$ ratio to 3.08271 (Nier, 1937). Based on blank runs ($n = 2$) analyzed together with samples, the total procedural blanks were about 0.8–1 pg for Re and 0.3–0.5 pg for Os. The Re and Os contents and the $^{187}\text{Os}/^{188}\text{Os}$ ratio of the analyzed in-house standard (JCBY) were 37.52 ± 0.11 ppb, 15.42 ± 0.05 ppb and 0.3363 ± 0.0005 , respectively (Table 8), consistent with the reference values of 38.61 ± 0.54 ppb, 16.23 ± 0.17 ppb, and 0.3363 ± 0.0029 (Du et al., 2012). The 2 sigma errors in $^{187}\text{Re}/^{188}\text{Os}$ ratios include uncertainties in spike calibration, decay constant uncertainties, and uncertainties in mass spectrometry measurements (in both run precision and isotope fractionation correction). The 2 sigma errors in the $^{187}\text{Os}/^{188}\text{Os}$ ratio are based on uncertainties in mass spectrometry measurements (in both run precision and isotope fractionation correction). Re-Os isotopic data were processed, plots constructed, and Re-Os isochron ages (Model 3 fit) calculated using the Isoplot program version 4.15 (Ludwig, 2012). Initial γOs values were calculated using the ^{187}Re decay constant of $1.666 \times 10^{-11} \text{ a}^{-1}$ (Smoliar et al., 1996) and the average initial solar system $^{187}\text{Re}/^{188}\text{Os}$ and $^{187}\text{Os}/^{188}\text{Os}_{(i)}$ ratios of 0.40186 and 0.09517, respectively (Shirey and Walker, 1998; Archer et al., 2014).

4. Analytical results

4.1. The Lomalampi PGE-(Ni-Cu) deposit

No direct age determination of the Lomalampi PGE-(Ni-Cu) deposit is available but its host rocks have been correlated with the komatiitic to picritic magmatism of the Savukoski Group (Törmänen et al., 2016), which has been dated by the Sm-Nd method at 2056 ± 25 Ma (Hanski et al., 2001b). Eight chromite separates from olivine cumulates contain 0.50–61.50 ppb Re and 4.77–19.36 ppb Os (Fig. 4) and show

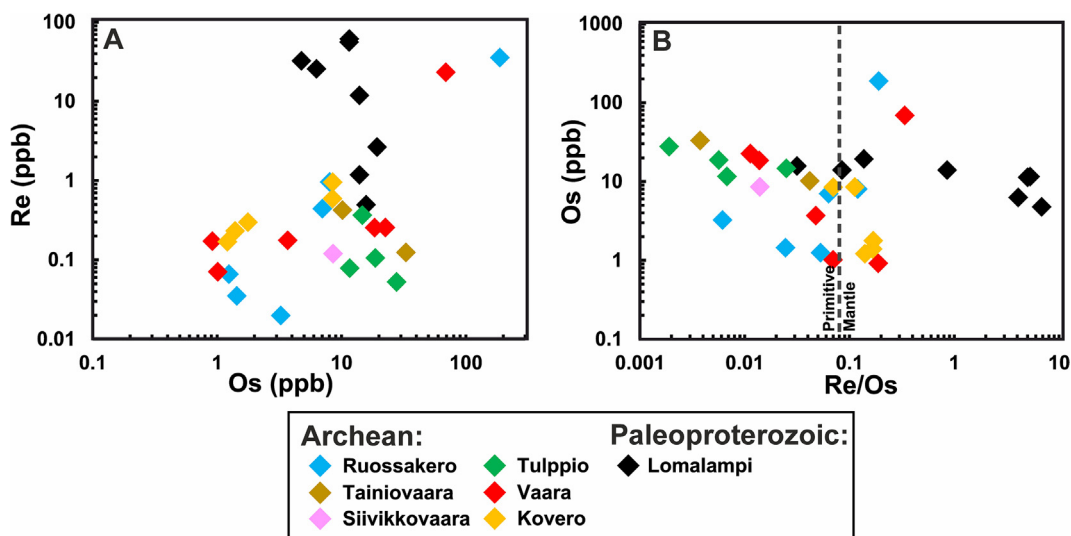


Fig. 4. Common Os vs. Re (A) and Re/Os ratio vs. Os (B) diagrams in log-log scale for chromite separates. Primitive mantle values of 3.4 ppb for Os and 0.28 ppb for Re and 0.08 for Re/Os taken from McDonough and Sun (1995).

$^{187}\text{Re}/^{188}\text{Os}$ ratios from 0.152 to 25.4 (Table 3). They have $^{187}\text{Os}/^{188}\text{Os}$ ranging from 0.1202 to 1.1866. In the age calculations, samples LOM-1, LOM-2 and LOM-4 were rejected because of a low signal and high Re/Os of > 1 . The Re-Os isotope data on four chromite separates with low Re/Os are aligned in the Re-Os isochron diagram, yielding an age of 2058 ± 93 Ma (Fig. 6a) and a near-chondritic initial $^{187}\text{Os}/^{188}\text{Os}$ ratio of 0.1139 ± 0.0028 corresponding to a γOs value of $+0.9 \pm 0.02$ (γOs is defined as the percentage deviation in $^{187}\text{Os}/^{188}\text{Os}$ from chondritic mantle at the time of interest). These results are consistent with the near-chondritic initial ratios obtained earlier for chromite separates from komatiites of the Jeesiörova area (Gangopadhyay et al., 2006). Three of these near-chondritic compositions were obtained from non-mineralized drillcore intervals and one from a mineralized interval.

The other four chromite samples with higher Re/Os ratios are from mineralized rocks and produced widely varying $\gamma\text{Os}(2050\text{ Ma})$ values from -96.9 to $+23.6$ (Table 3). Some of this variation could be explained by the occurrence of base metal sulfide inclusions in chromite grains (Fig. 3a) or pervasive alteration of the samples.

Two bulk-sulfide samples from the mineralized olivine cumulates have relatively high Re concentrations of 34.60 and 39.82 ppb and low

Os concentrations of 5.34 and 0.68 ppb Os (Fig. 5a). The corresponding $^{187}\text{Re}/^{188}\text{Os}$ ratios are high, 30.0 and 281.7 (Fig. 7) and the Os isotopic compositions radiogenic with $^{187}\text{Os}/^{188}\text{Os}$ ratios of 1.5331 and 9.4991, respectively. As shown by Fig. 6b, a two-point bulk-sulfide isochron gives an age of 1870 ± 22 Ma, falling in the range of the age of the Svecofennian orogeny, which occurred in several stages between 1.92 and 1.79 Ga (Lahtinen et al., 2005).

Three whole-rock black schist samples from the Lomalampi area yielded Re concentrations of 52.33–86.47 ppb, Os concentrations of 0.72–1.66 ppb, and high Re/Os ratios of 52.2–72.7 (Table 3 and Fig. 5). Their $^{187}\text{Re}/^{188}\text{Os}$ ratios range from 242.0 to 347.1 and $^{187}\text{Os}/^{188}\text{Os}$ ratios from 7.457 to 11.679, yielding highly variable $\gamma\text{Os}(2050\text{ Ma})$ values from -943 ± 260 to $+252 \pm 231$. The studied black schist samples give a highly uncertain Re-Os errorchron age estimation of 2059 ± 8900 Ma (Fig. 6c).

4.2. The Ruossakero Ni-(Cu) deposit

Six chromite separates from olivine cumulates of the Ruossakero deposit have Re concentrations of 0.02–35.74 ppb and Os

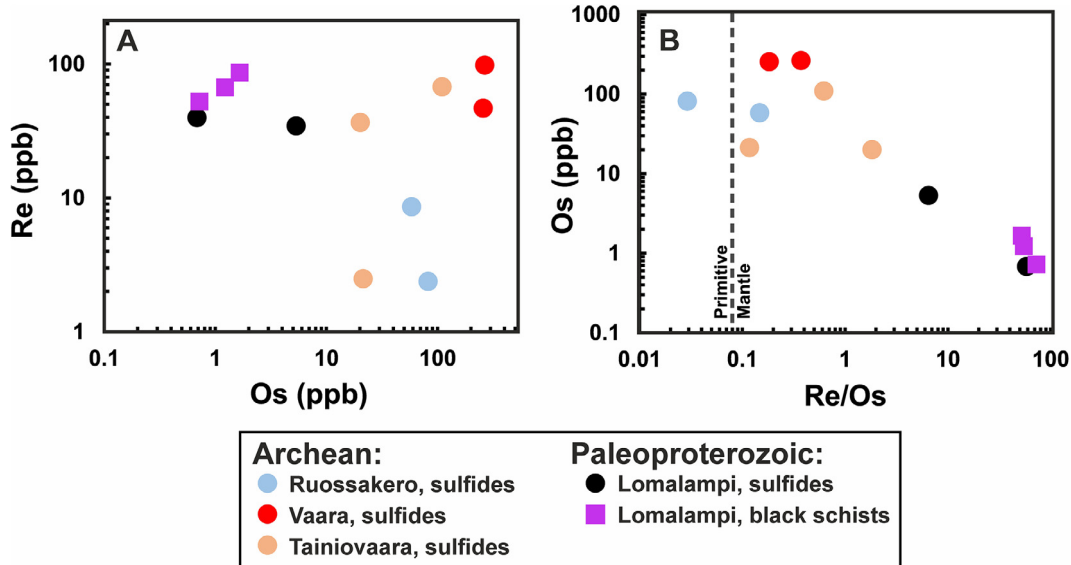


Fig. 5. Common Os vs. Re (A) and common Os vs. Re/Os ratio (B) diagrams in log-log scale for bulk-sulfide samples and country-rock black schists.

Table 3

Rhenium and osmium isotopic and compositional data for the Lomalampi deposit. T_{MA} and T_{RD} model ages in Ma. Highly erroneous (e.g., negative) T_{MA} and T_{RD} model ages are ignored. Initial γOs values were calculated assuming an age of 2050 Ma (Hanski et al., 2001b). Abbreviations: (D) = duplicate sample, Min = separated mineral, CRT = chromite, SUL = sulfide, loc = location, DH = drillhole, loc = sulfide, BS = black schist. Errors are in 2 sigma.

Sample	DH and depth	Loc.	Min.	Re (ppb)	Os (ppb)	$^{187}\text{Re}/^{188}\text{Os}$	$^{187}\text{Os}/^{188}\text{Os}$	$^{187}\text{Os}_{(I)}/^{188}\text{Os}_{(I)}$	γOs	T_{MA}	T_{RD}	Re/Os
LOM-1	LOM-407 52.50-55.50	Lomalampi mineralized	CRT	32.56 ± 0.25	4.77 ± 0.04	33.05556 ± 0.3432	1.1866 ± 0.0020	0.0381	-66.2 ± 30	1917 ± 61	6.83	
LOM-2	LOM-407 61.25-64.25	Lomalampi mineralized	CRT	61.5 ± 0.53	11.59 ± 0.10	25.3924 ± 0.2886	0.8857 ± 0.0044	0.0035	-96.9 ± 23.7	1795 ± 57	5.3	
LOM-2 (D)	LOM-407 61.25-64.25	Lomalampi mineralized	CRT	59.01 ± 0.44	11.35 ± 0.09	25.1401 ± 0.2548	0.8919 ± 0.0022	0.0184	-83.7 ± 22.9	1828 ± 58	5.2	
LOM-3	LOM-407 41.00-43.20	Lomalampi mineralized	CRT	11.93 ± 0.09	13.97 ± 0.11	4.13240 ± 0.0428	0.2582 ± 0.0004	0.1146	+1.5 ± 3.8	2074 ± 66	0.85	
LOM-4	LOM-406 8.00-11.00	Lomalampi mineralized	CRT	25.69 ± 0.11	6.30 ± 0.02	19.7235 ± 0.2079	0.8248 ± 0.0012	0.1395	+23.6 ± 18.0	2130 ± 67	4.08	
LOM-5	LOM-403 74.00-76.55	Lomalampi non-mineralized	CRT	1.18 ± 0.004	13.98 ± 0.04	0.4092 ± 0.0041	0.1272 ± 0.0002	0.113	+0.1 ± 0.4	1959 ± 62	0.08	
LOM-6	LOM-409 50.00-52.80	Lomalampi non-mineralized	CRT	0.50 ± 0.002	15.78 ± 0.05	0.1522 ± 0.0016	0.1202 ± 0.0002	0.115	+1.8 ± 0.2	1602 ± 51	1000 ± 33	
LOM-7	LOM-410 44.15-48.05	Lomalampi non-mineralized	CRT	2.66 ± 0.01	19.36 ± 0.06	0.66389 ± 0.0068	0.1368 ± 0.0002	0.1137	+0.7 ± 0.6	2197 ± 70	0.14	
LOM-1_S	LOM-407_S 61.25-64.25	Lomalampi mineralized	SUL	39.82 ± 0.12	0.68 ± 0.03	281.6588 ± 2.8899	9.4991 ± 0.0302	-0.2865	-353.7 ± 256.9	1968 ± 62	58.29	
LOM-2_S	LOM-407_S 52.50-55.50	Lomalampi mineralized	SUL	34.60 ± 0.10	5.34 ± 0.04	29.9934 ± 0.3534	1.5331 ± 0.0152	0.4911	+334.9 ± 30.8	2787 ± 88	6.48	
LOM-4_WR	LOM-439 76.20-76.30	Lomalampi black schist	BS	67.07 ± 0.20	1.22 ± 0.02	242.0210 ± 4.4630	7.4570 ± 0.0913	-0.9515	-942.7 ± 260.3	1794 ± 57	54.79	
LOM-5_WR	LOM-406_B 56.35-59.65	Lomalampi black schist	BS	52.33 ± 0.15	0.72 ± 0.03	347.1077 ± 3.5873	11.6787 ± 0.0299	-0.3808	-437.3 ± 316.3	1967 ± 62	72.66	
LOM-3_WR	LOM-406_A 56.35-59.65	Lomalampi black schist	BS	86.47 ± 0.64	1.66 ± 0.01	253.8495 ± 2.6372	9.2169 ± 0.0142	0.3974	+252.0 ± 231	2115 ± 67	52.24	

concentrations of 1.25–188.17 ppb, with the highest Re and Os contents determined for chromite separates from mineralized drillcore intervals. The $^{187}\text{Re}/^{188}\text{Os}$ ratios vary from 0.0297 to 0.9159 (Fig. 4) and $^{187}\text{Os}/^{188}\text{Os}$ ratios from 0.1068 to 0.1504. The Re-Os data on chromite separates from the Ruossakero deposit yield a Re-Os errorchron with an age of 2990 ± 750 Ma (Fig. 6f) with a near-chondritic initial $^{187}\text{Os}/^{188}\text{Os}$ ratio of 0.1010 ± 0.0062. Though being highly imprecise, this date is consistent with the U-Pb zircon age of 2930 Ma determined for felsic volcanic rocks in the Sarvisoja area (Karinen et al., 2015). One chromite separate with a near-chondritic γOs value (−1.4) at 2930 Ma from the Ruossakero deposit gives a T_{RD} model age of 2942 ± 97 Ma (the time of Re depletion determined from the intersection of the evolution of the sample assuming Re/Os = 0 and chondritic mantle evolution, representing a minimum age of Re depletion; Shirey and Walker, 1998). The initial γOs values of the chromite separates calculated at 2.93 Ga vary between −8.8 and −1.4, averaging −5.1 (Table 4). There are no systematic differences in γOs (2930 Ma) between chromite separates from mineralized and non-mineralized intervals.

Two bulk-sulfide separates from a mineralized olivine cumulate show 2.38 and 8.61 ppb Re and 82.01 and 58.49 ppb Os (Fig. 5). The corresponding $^{187}\text{Re}/^{188}\text{Os}$ ratios are 0.1391 and 0.7108 and $^{187}\text{Os}/^{188}\text{Os}$ ratios 0.1186 and 0.1466, yielding a two-point errorchron age of 2873 ± 60 Ma (Fig. 6g), with an initial $^{187}\text{Os}/^{188}\text{Os}$ ratio of 0.11178 ± 0.00034 and initial γOs of $+4.3 \pm 0.05$. Using the age of 2930 Ma, similar slightly suprachondritic γOs values, +4.6 and +4.0, are obtained for the two samples.

4.3. The Tulppio Dunite and related Ni-PGE mineralization

Four chromite samples from the olivine cumulate of the Tulppio Dunite, representing non-mineralized intervals of drillcore, show Re and Os concentrations of 0.05–0.37 ppb and 11.64–27.73 ppb (Figs. 4 and 5), and $^{187}\text{Re}/^{188}\text{Os}$ ratios of 0.0092–0.1200, respectively. No direct age determinations are available from the Tulppio greenstone belt; therefore, we use the age 2.82 Ga for γOs calculations, representing a lower age limit for komatiites in the Kuhmo greenstone belt in eastern Finland (Huhma et al., 2012a). The $^{187}\text{Os}/^{188}\text{Os}$ ratios vary between 0.1086 and 0.1145 yielding near-chondritic γOs (2820 Ma) values between −0.2 and +1.6 (Table 5). The obtained Re-Os isotope data did not yield any reasonable isochron due to a limited variation in $^{187}\text{Re}/^{188}\text{Os}$. The T_{MA} model ages (the time of separation from mantle determined from the intersection of the evolution of the sample and that of chondritic mantle; Shirey and Walker, 1998) calculated for chromite separates range from 2575 to 2871 Ma. On the other hand, the calculated T_{RD} model ages imply that the Tulppio Dunite has a minimum age of 2680 ± 88 Ma.

4.4. The Vaara Ni-(Cu-PGE) deposit

Six chromite samples from olivine/pyroxenite cumulates of the Vaara deposit have 0.07–23.24 ppb Re and 0.92–69.02 ppb Os (Figs. 4 and 5). The $^{187}\text{Re}/^{188}\text{Os}$ ratios vary from 0.0548 to 1.6269 and $^{187}\text{Os}/^{188}\text{Os}$ ratios from 0.1103 to 0.1827. The obtained Re-Os data on chromite separates (five of six; sample KOM-5 was left out because of its low signal) from the Vaara deposit yield an isochron with an age of 2719 ± 140 Ma (Fig. 6d) with a near-chondritic initial $^{187}\text{Os}/^{188}\text{Os}$ ratio of 0.1070 ± 0.0019 and γOs of -1.2 ± 0.02 . The chromite Re-Os isochron age is consistent with a previous age estimate of the Vaara deposit, 2771 ± 8 Ma, which is based on the U-Pb zircon age of a felsic enclave in a komatiite rock (Papunen et al., 2009). Assuming an age of 2820 Ma, the age of the Kuhmo greenstone belt komatiites (Huhma et al., 2012a), initial γOs for each chromite separate ranges from −7.6 to 0.0 (Table 6). There is no difference in the initial Os compositions between chromite separates from mineralized and non-mineralized drillcore intervals.

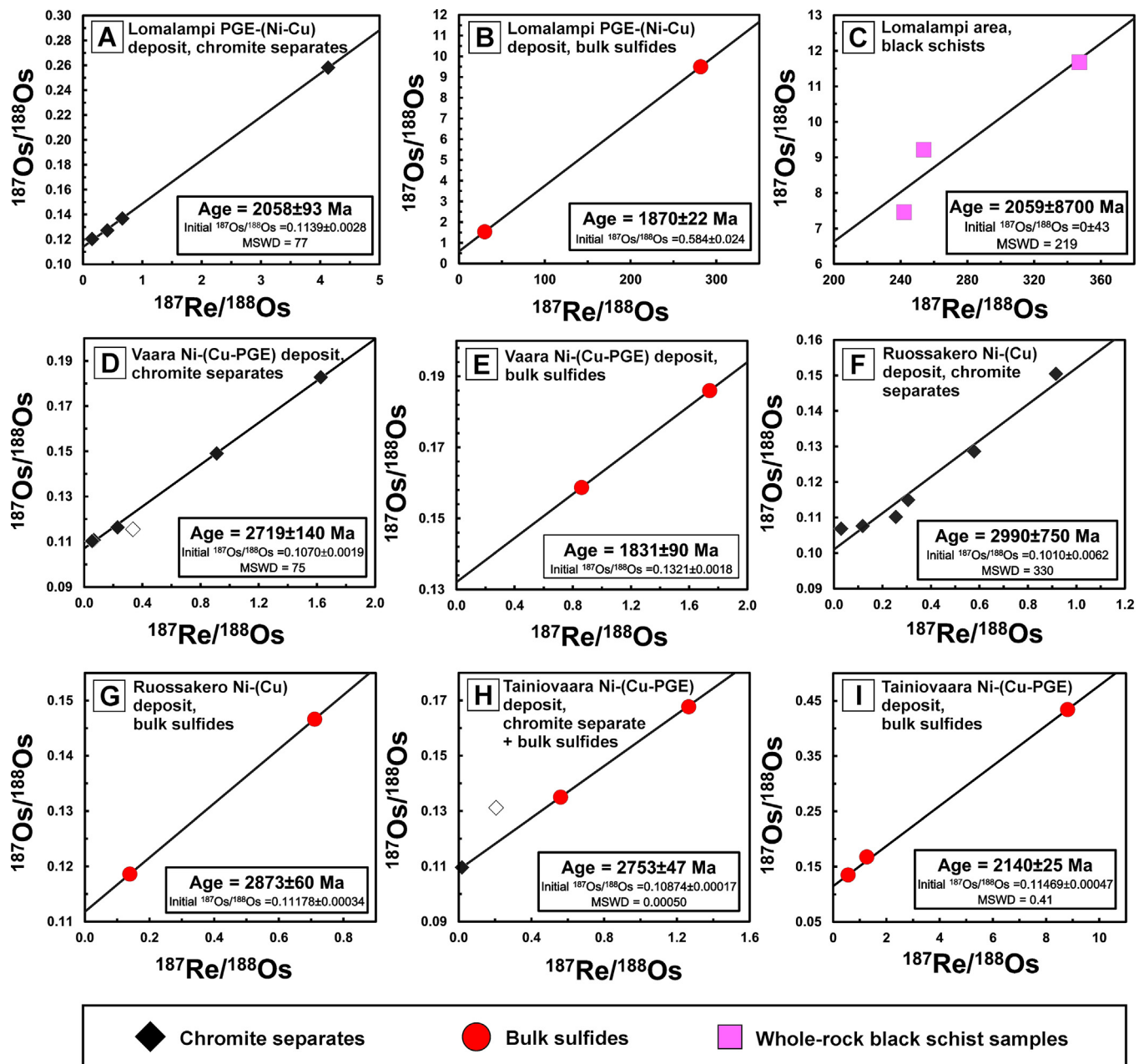


Fig. 6. Re-Os isochron diagrams for whole-rock samples and chromite and sulfide separates from the Lomalampi (A–C), Vaara (D–E), Ruossakero (F–G) and Tainiovaara (H–I) deposits. Disturbed samples are presented as open symbols and are not included in the isochron calculations.

Two bulk-sulfide samples from the olivine/pyroxene cumulate of the Vaara deposit contain 46.85 and 98.46 ppb Re. In our whole data set, the Vaara sulfides produce the highest Os concentrations (257.3 and 265.5 ppb). These two sulfide samples have $^{187}\text{Re}/^{188}\text{Os}$ ratios of 0.8604 and 1.7411 and $^{187}\text{Os}/^{188}\text{Os}$ ratios of 0.1587 and 0.1860, respectively, giving moderately positive (+9.1) and slightly negative (−4.9) $\gamma\text{Os}(2820\text{ Ma})$ values. Plotted on an isochron diagram (Fig. 6e), the two sulfide separates yield a Paleoproterozoic errorchron age of 1831 ± 90 Ma fitting with the age of the Svecofennian orogeny (Lahtinen et al., 2005).

4.5. The Tainiovaara Ni-(Cu-PGE) deposit

Two chromite separates from olivine cumulates of the Tainiovaara deposit, one from a non-mineralized and the other from a mineralized drillcore interval, gave Re concentrations of 0.12 and 0.43 ppb, Os

concentrations of 33.07 and 10.19 ppb (Figs. 4 and 5), and $^{187}\text{Re}/^{188}\text{Os}$ ratios of 0.0181 and 0.2016, respectively. The samples show different $^{187}\text{Os}/^{188}\text{Os}$ ratios of 0.1096 and 0.1312, yielding near-chondritic and suprachondritic γOs values of +1.1 and +13.0, respectively (Table 7), with the assumption of 2820 Ma for their age (Huhma et al., 2012a).

Three bulk-sulfide separates from a mineralized olivine cumulate contain 2.50–67.87 ppb Re and 20.13–109.86 ppb Os. Their $^{187}\text{Re}/^{188}\text{Os}$ varies from 0.5603 to 8.8049 and $^{187}\text{Os}/^{188}\text{Os}$ from 0.1350 to 0.4343, yielding a Re-Os isochron age of 2140 ± 25 Ma, apparently as a result of resetting, particularly sample TAI-3_S.

The obtained Re-Os data of the chromite separates from the Tainiovaara deposit did not give a reasonable isochron. Therefore, we used the least altered non-mineralized chromite sample (TAI-1) and two bulk-sulfide analyses (TAI-1_S and duplicate analysis) to estimate the magmatic age of the ultramafic body, resulting in a three-point isochron with an age of 2753 ± 47 Ma (Fig. 6h) and a near-chondritic initial

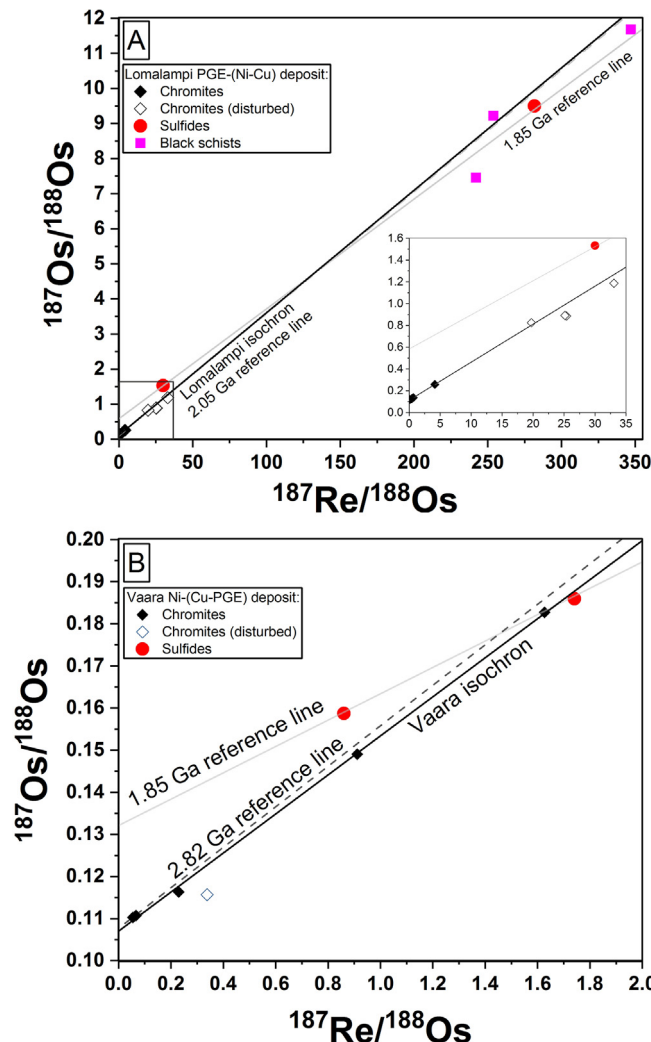


Fig. 7. A) Re-Os isochron diagram for samples from the Lomalampi PGE-(Ni-Cu) deposit with 2.05 Ga (dashed) and 1.85 Ga reference lines (initial $^{187}\text{Os}/^{188}\text{Os} = 0.584$). B) Re-Os isocron for the Vaara Ni-(Cu-PGE) deposit with 2.82 Ga (dashed) and 1.85 Ga reference lines (initial $^{187}\text{Os}/^{188}\text{Os} = 0.1321$).

$^{187}\text{Os}/^{188}\text{Os}$ ratio of 0.10874 ± 0.00017 and γ_{Os} of $+0.7 \pm 0.01$. Given the general open behavior of sulfides in the studied altered ultramafic rocks this age should be regarded with caution. Nevertheless, due to the low $^{187}\text{Re}/^{188}\text{Os}$ ratio, the initial ratios are close to chondritic for the chromite and two sulfide samples even though the age of 2820 Ma were used.

4.6. Non-mineralized komatiites from the Siivikkovaara and Kovero areas

A chromite separate obtained from a komatiitic ultramafic rock in the Siivikkovaara area, Archean Kuhmo greenstone belt, contains 0.12 ppb Re and 8.58 ppb Os and its $^{187}\text{Re}/^{188}\text{Os}$ and $^{187}\text{Os}/^{188}\text{Os}$ ratios are 0.0675 and 0.1095, respectively. Huhma et al. (2012b) conducted whole-rock Sm-Nd dating of komatiites and komatiitic basalts from the same area and got an imprecise Sm-Nd isochron age of 2827 ± 190 Ma, while for a felsic porphyry dike cutting komatiites in the area, Huhma et al. (2012a) obtained a U-Pb zircon age of 2795 ± 3 Ma. A mafic sill cutting komatiites ~40 km north of Siivikkovaara yielded an age of 2823 ± 6 Ma (Huhma et al. 2012a). Based on these results, we assume that the age of the Siivikkovaara komatiites is ca. 2820 Ma. Using this age, we obtained a near-chondritic γ_{Os} value of -1.2 for the analyzed chromite separate (Table 8).

Four chromite separates from highly altered non-mineralized

Table 4
 Rhenium and osmium isotopic and compositional data for the Ruossakero deposit. Initial γ_{Os} values were calculated assuming an age of 2930 Ma determined for associated felsic volcanic rocks (Karinen et al., 2015). Errors are in 2 sigma.

Sample id	DH and depth	Loc.	Min.	Re (ppb)	Os (ppb)	$^{187}\text{Re}/^{188}\text{Os}$	$^{187}\text{Os}/^{188}\text{Os}_{(0)}$	γ_{Os}	T_{MA}	T_{RD}	Re/Os
RUO-1	RUO-416 25.45-28.45	Ruossakero non-mineralized	CRT	0.96 \pm 0.01	8.03 \pm 0.06	0.5783 \pm 0.0059	0.1286 \pm 0.0003	0.0997	-6.6 \pm 0.7	543 \pm 17	0.12
RUO-2	RUO-416 69.15-72.00	Ruossakero non-mineralized	CRT	0.02 \pm 0.0002	3.25 \pm 0.02	0.0297 \pm 0.0004	0.1068 \pm 0.0002	0.1053	-1.4 \pm 0.2	3171 \pm 100	2942 \pm 97
RUO-3	RUO-417 102.00-105.00	Ruossakero non-mineralized	CRT	0.04 \pm 0.0003	1.44 \pm 0.01	0.1187 \pm 0.0013	0.1076 \pm 0.0005	0.1017	-4.8 \pm 0.5	3980 \pm 126	2831 \pm 93
RUO-3 (D)	RUO-417 102.00-105.00	Ruossakero non-mineralized	CRT	0.07 \pm 0.001	1.25 \pm 0.01	0.2556 \pm 0.0026	0.1101 \pm 0.0008	0.0973	-8.8 \pm 0.8	6556 \pm 208	2469 \pm 81
RUO-4	RUO-434 101.65-104.65	Ruossakero mineralized	CRT	35.74 \pm 0.30	188.17 \pm 1.42	0.9159 \pm 0.0099	0.1504 \pm 0.0002	0.1046	-2.0 \pm 1.1	2677 \pm 85	0.19
RUO-5	RUO-413 171.20-174.20	Ruossakero mineralized	CRT	0.44 \pm 0.003	7.01 \pm 0.05	0.3058 \pm 0.0031	0.1149 \pm 0.0002	0.0996	-6.7 \pm 0.4	7100 \pm 225	1775 \pm 58
RUO-1_S	RUO-413 107.00-110.00	Ruossakero mineralized	SUL	8.61 \pm 0.03	58.49 \pm 0.20	0.7108 \pm 0.0073	0.1466 \pm 0.0004	0.1111	+4.0 \pm 0.9	3697 \pm 117	0.15
RUO-2_S	RUO-434 185.60-188.60	Ruossakero mineralized	SUL	2.38 \pm 0.01	82.01 \pm 0.26	0.1391 \pm 0.0014	0.1186 \pm 0.0002	0.1116	+4.6 \pm 0.3	1889 \pm 60	1242 \pm 41

Table 5
Rhenium and osmium isotopic and compositional data for the Tulppio Dunite. Initial γ Os values were calculated using an age of 2820 Ma (Huhma et al., 2012a). Errors are in 2 sigma.

Sample id	DH and depth	Loc.	Min.	Re (ppb)	Os (ppb)	$^{187}\text{Re}/^{188}\text{Os}$	$^{187}\text{Os}/^{188}\text{Os}$	$^{187}\text{Os}/^{188}\text{Os}_{\text{f}}$	γ Os	T _{MA}	T _{RD}	Re/Os
TUL-1	TUL-307 47.00-49.60	Tulppio non-mineralized	CRT	0.08 ± 0.0003	11.64 ± 0.04	0.0327 ± 0.0003	0.11081 ± 0.0002	0.1092	+1.6 ± 0.2	2575 ± 82	2369 ± 78	0.01
TUL-2	TUL-314 73.90-76.90	Tulppio non-mineralized	CRT	0.37 ± 0.02	14.73 ± 0.05	0.1200 ± 0.0073	0.1145 ± 0.0004	0.1087	+1.1 ± 0.5	2607 ± 83	1840 ± 60	0.02
TUL-3	TUL-320 5.20-8.20	Tulppio non-mineralized	CRT	0.05 ± 0.001	27.73 ± 0.08	0.0092 ± 0.0002	0.1088 ± 0.0002	0.1084	+0.8 ± 0.1	2719 ± 86	2638 ± 87	0.002
TUL-4	TUL-320 98.40-101.40	Tulppio non-mineralized	CRT	0.11 ± 0.001	18.76 ± 0.06	0.0273 ± 0.0003	0.1086 ± 0.0002	0.1073	-0.2 ± 0.1	2871 ± 91	2680 ± 88	0.01

Table 6
Rhenium and osmium isotopic and compositional data for the Vaara deposit. Initial γ Os values were calculated assuming an age of 2820 Ma (Huhma et al., 2012a). Errors are in 2 sigma.

Sample id	DH and depth	Loc.	Min.	Re (ppb)	Os (ppb)	$^{187}\text{Re}/^{188}\text{Os}$	$^{187}\text{Os}/^{188}\text{Os}$	$^{187}\text{Os}/^{188}\text{Os}_{\text{f}}$	γ Os	T _{MA}	T _{RD}	Re/Os
VAA-1	VAA-631 77.15-79.30	Vaara non-mineralized	CRT	0.18 ± 0.001	3.70 ± 0.03	0.2299 ± 0.0024	0.1163 ± 0.0002	0.1053	-2.1 ± 0.3	3615 ± 115	1574 ± 52	0.05
VAA-2	VAA-631 103.95-106.95	Vaara non-mineralized	CRT	0.25 ± 0.002	18.51 ± 0.14	0.0665 ± 0.0007	0.1107 ± 0.0002	0.1075	0.0 ± 0.2	2850 ± 90	2388 ± 78	0.01
VAA-3	VAA-654 41.70-44.90	Vaara non-mineralized	CRT	0.26 ± 0.002	22.58 ± 0.17	0.0548 ± 0.0006	0.1103 ± 0.0002	0.1076	+0.1 ± 0.2	2827 ± 90	2449 ± 80	0.01
VAA-4	VAA-656 50.00-53.00	Vaara mineralized	CRT	23.24 ± 0.21	69.02 ± 0.52	1.6269 ± 0.0184	0.1827 ± 0.0003	0.1045	-2.8 ± 1.8	2671 ± 85		0.34
KOM-5	M4513988635 28.8-31.1	Vaara non-mineralized	CRT	0.07 ± 0.001	1.01 ± 0.01	0.3381 ± 0.0035	0.1157 ± 0.0004	0.0994	-7.6 ± 0.5		1670 ± 55	0.07
KOM-6	M4513988635 34.6-35.85	Vaara non-mineralized	CRT	0.17 ± 0.001	0.92 ± 0.01	0.9116 ± 0.0094	0.1490 ± 0.0005	0.1052	-2.2 ± 1.1	2539 ± 80		0.19
VAA-1_S	VAA-656 101.50-104.90	Vaara mineralized	SUL	98.46 ± 0.73	265.54 ± 2.48	1.7411 ± 0.0197	0.1860 ± 0.0010	0.1022	-4.9 ± 2.1	2587 ± 82		0.37
VAA-2_S	VAA-633 90.8.00	Vaara mineralized	SUL	46.85 ± 0.35	257.32 ± 2.58	0.8604 ± 0.0100	0.1587 ± 0.0007	0.1173	+9.1 ± 1.2	4012 ± 127		0.18

Table 7

Rhenium and osmium isotopic and compositional data for the Tainiovaara deposit. Initial γ Os values were calculated assuming an age of 2820 Ma (Huhma et al., 2012a). Errors are in 2 sigma.

Sample id	DH and depth	Loc.	Min.	Re (ppb)	Os (ppb)	$^{187}\text{Re}/^{188}\text{Os}$	$^{187}\text{Os}/^{188}\text{Os}$	$^{187}\text{Os}/^{188}\text{Os}_{\text{SI}}$	γ Os	T_{MA}	T_{RD}	Re/Os	
TAI-1	TAI-311 17.85-20.85	Tainiovaara non-mineralized	CRT	0.12 ± 0.001	33.07 ± 0.25	0.0181 ± 0.0002	0.1096 ± 0.0002	0.1087 ± 0.0002	+1.1 ± 0.2	2664 ± 84	2546 ± 84	0.004	
TAI-2	TAI-303 53.25-56.25	Tainiovaara mineralized	CRT	0.43 ± 0.003	10.19 ± 0.08	0.2016 ± 0.0021	0.1312 ± 0.0011	0.1215 ± 0.0011	+13.0 ± 1.0	0.04	-90 ± 9.7	2156 ± 68	1.82
TAI-3_S	TAI-304 92.30-95.50	Tainiovaara mineralized	SUL	36.69 ± 0.32	20.13 ± 0.15	8.8049 ± 0.0977	0.4343 ± 0.0007	0.0107 ± 0.0007	-0.6 ± 27.5	2771 ± 88	0.62	0.05 ± 0.7	
TAI-1_S	TAI-307 47.40-50.40	Tainiovaara mineralized	SUL	67.87 ± 0.50	109.86 ± 4.27	1.2645 ± 0.6133	0.1678 ± 0.0002	0.1069 ± 0.0002	+0.5 ± 0.7	2967 ± 94	0.12	0.2503 ± 0.003	
TAI-1_S (D)	TAI-307 47.40-50.40	Tainiovaara mineralized	SUL	2.50 ± 0.01	21.36 ± 0.07	0.5603 ± 0.0057	0.1350 ± 0.0003	0.1081 ± 0.0003	+0.5 ± 0.7	2967 ± 94	0.12	0.2503 ± 0.003	

Table 8

Rhenium and osmium isotopic and compositional data for chromite from the Kovero and Siivikkovaara area together with analytical data for a reference standard and blank. Initial γ Os values were calculated assuming an age of 2820 Ma (Huhma et al., 2012a). Abbreviations: ID = sample id, (D) = duplicate sample, Min = separated mineral, Min = standard = in-house standard (JCBY), CRT = chromite. Errors are in 2 sigma.

Sample id	DH and depth	Loc.	Min.	Re (ppb)	Os (ppb)	$^{187}\text{Re}/^{188}\text{Os}$	$^{187}\text{Os}/^{188}\text{Os}$	$^{187}\text{Os}/^{188}\text{Os}_{\text{SI}}$	γ Os	T_{MA}	T_{RD}	Re/Os	
KOM-1	E/KOV-010 13.5-14.5	Kovero non-mineralized	CRT	0.17 ± 0.001	1.21 ± 0.01	0.6810 ± 0.0072	0.1239 ± 0.0008	0.0912 ± 0.0008	-15.2 ± 1.0	0.14	-23.0 ± 1.1	0.17	
KOM-2	E/KOV-010 14.5-15.7	Kovero non-mineralized	CRT	0.23 ± 0.002	1.40 ± 0.01	0.8011 ± 0.0082	0.1213 ± 0.0007	0.0828 ± 0.0007	-22.2 ± 1.1	0.17	-22.2 ± 1.1	0.17	
KOM-2 (D)	E/KOV-010 14.5-15.7	Kovero non-mineralized	CRT	0.30 ± 0.004	1.77 ± 0.01	0.8131 ± 0.0134	0.1228 ± 0.0004	0.0837 ± 0.0004	+16.9 ± 9.3	0.07	+16.9 ± 9.3	0.07	
KOM-3	E/KOV-02 7-8.5	Kovero non-mineralized	CRT	0.59 ± 0.004	8.50 ± 0.11	0.3451 ± 0.0070	0.1423 ± 0.0100	0.1257 ± 0.0100	-24.6 ± 1.3	0.11	-24.6 ± 1.3	0.11	
KOM-4	E/KOV-02 12.9-13.8	Kovero non-mineralized	CRT	0.96 ± 0.01	8.53 ± 0.07	0.5457 ± 0.0061	0.1074 ± 0.0013	0.0811 ± 0.0013	-1.2 ± 0.2	3056 ± 97	2862 ± 94	0.01	
KOM-8	KH/SU-005 83-83.5, 84.8-85.8	Siivikkovaara non-mineralized	Standard	37.52 ± 0.11	15.42 ± 0.05	11.8402 ± 0.1199	0.3363 ± 0.0005	0.1063 ± 0.0002	0.3363 ± 0.0005	-	2554 ± 84	0.01	-
JCBY			Blank	0	0	7.1008 ± 0.1274	0.2309 ± 0.0035	0.2331 ± 0.0030	0.2331 ± 0.0030	-	-	-	
BK			Blank	0	0	16.7335 ± 0.2549	0.2331 ± 0.0030	0.2331 ± 0.0030	0.2331 ± 0.0030	-	-	-	

olivine cumulates from the Kovero area, Archean Kovero greenstone belt, have $0.17\text{--}0.96$ ppb Re, $1.21\text{--}8.53$ Os (Figs. 4 and 5). Their $^{187}\text{Re}/^{188}\text{Os}$ ratios fall in the range of $0.3451\text{--}0.8131$, while $^{187}\text{Os}/^{188}\text{Os}$ ratios are in the range of $0.1074\text{--}0.1423$. These Re-Os data did not give any reasonable isochron and because of their relatively high $^{187}\text{Re}/^{188}\text{Os}$ and low, most of the model ages from chromite separates are negative. The T_{RD} model age for the chromite with the highest Os concentration is Archean, 2862 ± 94 Ma, which likely represents a minimum age for the komatiite (Table 8). Using the U-Pb zircon method, Huhma et al. (2012a) dated felsic volcanic rocks and gabbroic rocks from the Kovero greenstone belt, concluding that there are two age groups of rocks in the belt. The older group includes felsic volcanic rocks with an age of 2878 ± 2 Ma and the younger group contains felsic dike rocks and gabbroic rocks with ages of $2.75\text{--}2.76$ Ga. The age of the Kovero komatiites could be either ca. 2880 Ma (that of the older group) or 2820 Ma, i.e. around the same as that of the Siivikkovaara komatiites. Regardless of the assumed age, the calculated γOs values are variable, from -24.6 to $+16.9$ (at 2820 Ma) (Table 8). Given the highly altered nature of chromite at Kovero (see Fig. 3f), the large variation in the initial isotope ratios is not surprising.

5. Discussion

5.1. Role of metamorphism and alteration in resetting of the Re-Os isotope system

Post-magmatic resetting of sulfides has been observed in several Ni-Cu deposits worldwide. The Re-Os isotopes from the Voisey's Bay Ni-Cu-Co sulfide system define an isochron age of 1004 ± 20 Ma, which is significantly younger than the 1333 Ma age of Voisey's Bay magmatic system (Amelin et al., 2000; Lambert et al., 2000). Lambert et al. (2000) suggested a mineral-scale open-system behavior and disturbance of the Re-Os system during the orogenic event at ca. 1 Ga. Lahaye et al. (2001) also came to a similar conclusion based on the Re-Os isotopic study of the 2.7 Ga komatiitic flows and related Ni-Cu sulfide deposits at Alexo, Texmont and Hart in the Abitibi greenstone belt, suggesting re-equilibration of the Re-Os system during the Grenville orogeny at ca. 1.2 Ga when hydrothermal fluids remobilized Re and Os in the sulfides at a mineral scale.

Even though chromite is generally resistant to alteration processes and have high Os concentrations, making it a superb mineral for getting information of initial Os isotopic compositions of mafic to ultramafic magmas, sometimes it has been far from immune to post-magmatic processes. Some chromite separates from the Lomalampi, Ruossakero and Vaara deposits show negative γOs values, which suggests that these separates represent disturbed samples with Re gain or alternatively, they represent separates containing some sulfide impurities. The chromite separates from Archean komatiites of the Kovero area were almost totally altered to magnetite during metamorphic processes (Figs. 2e and 3f), and hardly no original textures of the rocks or minerals are preserved. Even though the Re and Os concentrations in the Kovero chromite samples are within the range of other studied chromite samples (Fig. 4), the high degree of alteration is reflected in their Re-Os isotope compositions, with the γOs values varying from clearly positive ($+16.9$) to negative (-24.6 to -15.2) (Fig. 8).

The bulk-sulfide separates from the Paleoproterozoic Lomalampi PGE-(Ni-Cu) deposit and the Archean Vaara Ni-(Cu-PGE) deposit give younger dates compared to the Re-Os isochron ages based on chromite samples, with the sulfide separates from both deposits plotting on a reference line of ca. 1.85 Ga (Fig. 7a,b). Some resetting can also be seen in the Re-Os isotope data on the bulk-sulfide separates from the Tainiovaara deposit. The 1.85 Ga date corresponds to the timing of the Svecofennian orogeny, which occurred in several stages between 1.92 and 1.79 Ga (Lahtinen et al., 2005). Some of the Lomalampi mineralized samples contain trace amounts of sulfarsenides (e.g., cobaltite, gersdorffite and arsenopyrite), nickeline, löllingite, pyrite, sphalerite,

millerite, galena and molybdenite, and also three different types of Pd-Ni-Te \pm Sb \pm Bi phases and sperrylite (PtAs_2) (Törmänen et al., 2016). Some of these mineral associations could represent minerals formed during metamorphic and/or hydrothermal processes, with their metals having been mobilized from original magmatic sulfides or from country rocks.

Similarly with the bulk sulfide separates from the Paleoproterozoic Lomalampi deposit, those of the Archean Vaara deposit indicate that they re-equilibrated during the Svecofennian orogenic events. Konnunaho et al. (2013) showed that in the Vaara deposit, post-magmatic modification of sulfides has occurred, including extensive replacement of sulfides with magnetite and concomitant loss of sulfur. In these processes, post-magmatic high-Ni minerals, such as millerite and some violarite, were formed.

Due to their highly radiogenic Os isotope compositions, black shales are notorious for the difficulty of getting reliable information on their initial Os isotope compositions, hampering the attempts to model the isotopic effects of magma-sediment interaction (e.g., Hanski et al., 2011). The situation becomes even more complex if the isotopic system of black shales have become open during metamorphic transformations. At Lomalampi, the black schist sample without visual sulfides gives a chondritic model age of ca. 2.1 Ga, but two other samples rich in sulfides yield younger model ages of ca. 1.8 and 2.0 Ga, indicating post-depositional resetting. It is interesting to note that Hanski et al. (2016) obtained an isochron age of 1848 ± 18 Ma for black shales associated with the Talvivaara Ni-Zn-Cu deposit in central Finland. This together with the results of our study indicates that sulfides in both black shales and magmatic Ni-Cu deposits have been widely reset isotopically during the Svecofennian orogeny in Finland, both in the Archean basement and Paleoproterozoic supracrustal belts.

5.2. The origin of parental magmas, sulfur source and signs of crustal contamination

Most of the Os isotope compositions of the chromite samples from the Archean Ruossakero, Vaara, Tainiovaara, and Tulppio deposits gave close-to-zero initial γOs values (Fig. 8). Also one reference chromite separate from the Archean Kuhmo greenstone belt (Siivikkovaara) shows a near-chondritic Os isotope composition. The same is true for the studied Paleoproterozoic komatiite magmatism in the Central Lapland greenstone and related PGE-(Ni-Cu) deposit at Lomalampi, showing near-chondritic γOs values (Gangopadhyay et al., 2006; this study). This indicates that their Os is derived overwhelmingly from a mantle source with a chondritic Re-Os isotope evolution and contamination of the magmas with crustally derived radiogenic osmium has been negligible. Some chromite separates from mineralized intervals of the Tainiovaara and Lomalampi deposits have positive γOs values ($+13.0 \pm 1$ and $+23.6 \pm 18$, respectively), indicating a minor/moderate degree of contamination.

The reference chromite separated from non-mineralized komatiitic rocks occurring in the Siivikkovaara area in the Archean Kuhmo greenstone belt shows near-chondritic γOs of -1.2 , which indicates that the respective magma was not contaminated with Archean crust. This is also supported by subchondritic LREE/HREE ratios of these rocks (Papunen et al., 2009) and their ϵ_{Nd} values, which are mostly positive though somewhat scattered due to metamorphic effects (Huhma et al., 2012b). Based on geochemical evidence, Maier et al. (2013) proposed that the Kuhmo komatiites were erupted on an oceanic plateau and have not interacted with old continental crustal material. This model is also favored by Puchtel et al. (1998b) for komatiites in the Kostomuksha greenstone belt on the Russian side of the border.

In the Archean Ruossakero and Tainiovaara deposits, the γOs values for bulk-sulfide samples are the following: Ruossakero $+4.0$ and $+4.6$ and Tainiovaara -0.6 , $+0.5$ and -90 (Tables 4 and 7, Fig. 9). Most of these values indicate very minor or no contamination with radiogenic Os-bearing crustal material. The Tainiovaara γOs value of -90 is

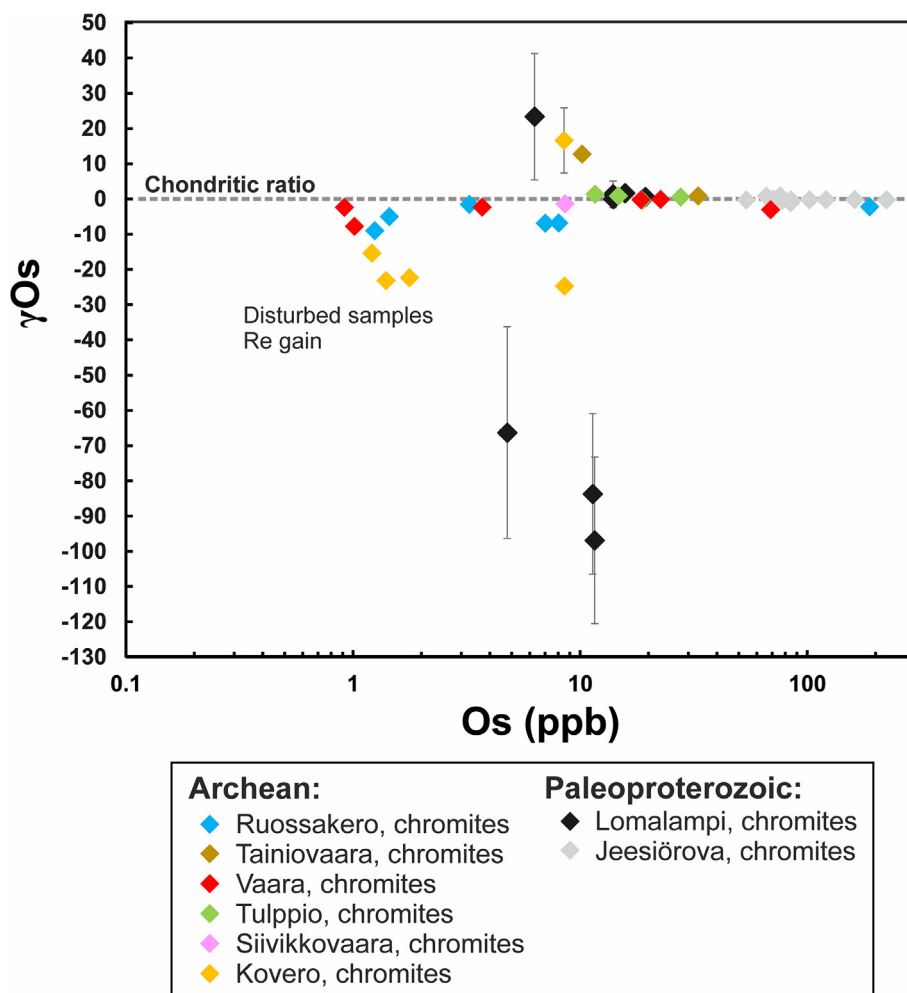


Fig. 8. Plot of common Os against γ_{Os} for chromite separates from komatiitic deposits. Also shown are compositions of chromite separates from Paleoproterozoic Jeesiörova komatiites taken from Gangopadhyay et al. (2006). Horizontal black line represents a chondritic reference composition with $\gamma_{\text{Os}} = 0$. Symbols with no error bars represent analytical results with errors smaller than or equal to the symbol size. Reference ages used for γ_{Os} calculations are 2050 Ma for Lomalampi and Jeesiörova, 2820 Ma for Tulppio, Vaara and Tainiovaara, and 2930 Ma for Ruossakero.

probably caused by disturbance of the sulfide sample due to gain of Re and the near-chondritic values -0.6 and $+0.5$ are most likely representative of the mantle source or alternatively, the contaminant had a low Os concentration and/or near-chondritic Os isotope composition. It is noteworthy that the country rocks around the Tainiovaara deposits are Archean upper crustal felsic gneisses likely having negligible Os contents, but contamination could have occurred at a greater depth, below surrounding gneisses. The bulk-sulfide samples from the Ruossakero deposit also show near-chondritic γ_{Os} values ($+4.0$ and $+4.6$).

Of the studied Archean deposits, only the Vaara deposit has earlier been studied for sulfur isotopes. For Ni-Cu ore samples, Konnunaho et al. (2013) measured $\delta^{34}\text{S}$ values from $+1.54$ to $+2.13\text{\textperthousand}$ and $\Delta^{33}\text{S}$ values from $+0.53$ to $+0.66\text{\textperthousand}$, while sulfide-bearing country rocks yielded $\delta^{34}\text{S}$ values between -1.8 and $+4.6\text{\textperthousand}$ and $\Delta^{33}\text{S}$ values from $+0.2$ to $+2.4\text{\textperthousand}$. The analyses revealed the presence of mass-independent fractionation of sulfur isotopes (MIF-S), both in the Ni-Cu deposit and its country rocks, indicating that crustal contamination and incorporation of crustal sulfur was an important process in the genesis of the Vaara deposit. The two bulk sulfide separates from the Vaara deposit show γ_{Os} values of -4.9 and $+9.1$ (Table 6 and Fig. 9). Given the high degree of modification of the sulfide assemblage due to post-magmatic oxidation and related loss of sulfur (Konnunaho et al., 2013), the initial ratios are rather close to chondritic and likely indicate that osmium is mostly magmatic in these sulfide samples. Other explanation is that the two isotopic systems are decoupled and the sulfur and the

osmium came from different sources, with one potential source being sediments and other the mantle. It thus seems that contamination which caused MIF-S did not significantly affect the Os isotope signature of the rocks, which implies that the Os concentration of the contaminant is low compared to that of the komatiitic magma.

The relatively homogenous, near-chondritic initial $^{187}\text{Os}/^{188}\text{Os}$ compositions of the bulk-sulfide samples from the studied Archean komatiitic deposits (excluding the most disturbed Tainiovaara sample with a γ_{Os} value of -90) indicate that osmium in sulfides was derived from a isotopically homogenous mantle source and the magma was not affected by contamination with radiogenic Os. This could be achieved if efficient magmatic collection of mantle-derived sulfide happened from a large volume of magma, which is plausible in mantle plume settings (Condie, 2001; Ripley and Li, 2013). Such a setting is likely for the studied komatiitic deposits (e.g., Puchtel and Humayun, 2005; Maier et al., 2013; Puchtel et al., 1998a, 2001, 2005). The mantle-like Os isotope signature in the sulfide samples could also be retained in spite of contamination processes, if the magma had a high Os content and externally derived sulfur came from a source with a low Os content, such as VMS mineralization (Bekker et al., 2009; Fiorentini et al., 2012).

In the case of the Paleoproterozoic Lomalampi PGE-(Ni-Cu) deposit, the two sulfide-bearing mineralized olivine cumulates sampled near black schist drillcore intervals show different γ_{Os} values at the magmatic age of 2050 Ma, one being highly radiogenic ($+335 \pm 31$) and

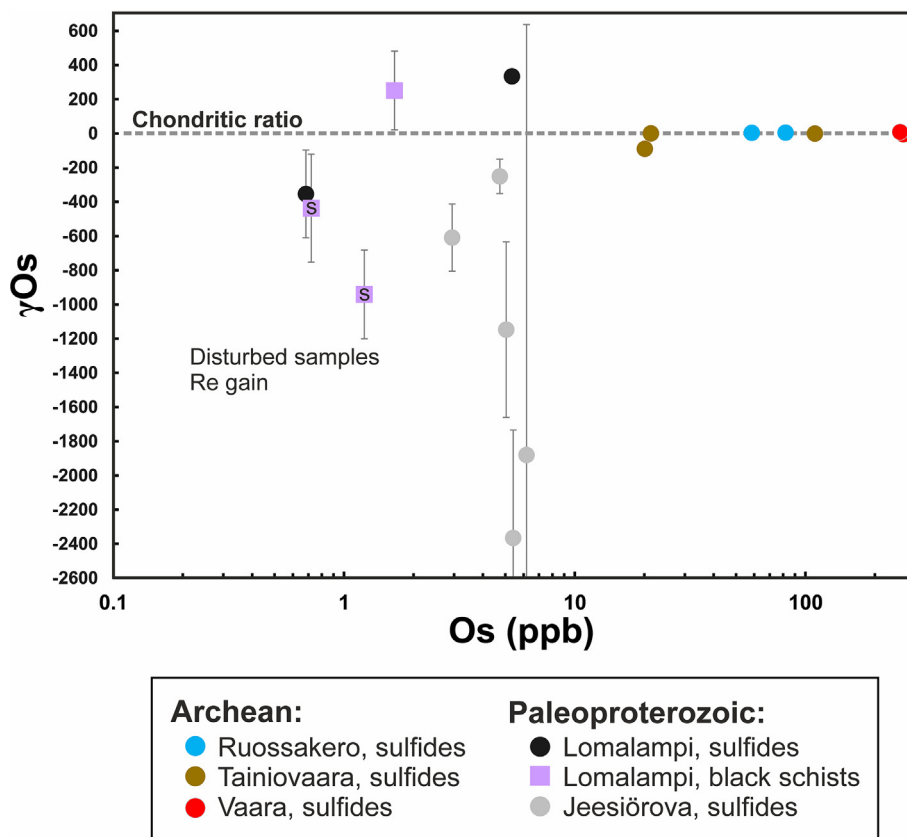


Fig. 9. Plot of common Os against initial γ Os values for bulk-sulfide samples from the studied komatiitic deposits and whole-rock black schist samples from the country rocks of the Lomalampi deposit, potential contaminants for the Lomalampi mineralization. The sulfide analyses from the Paleoproterozoic Jeesiörova komatiites are from Gangopadhyay et al. (2006). The horizontal black line represents a chondritic reference composition with γ Os = 0. Symbols with no error bars represent analytical results with errors smaller than or equal to the symbol size. The black schist symbols with letter s refer to sulfide-bearing samples. The ages used for γ Os calculations are 2050 Ma for Lomalampi and Jeesiörova, 2820 Ma for Tulppio, Vaara and Tainiovaara, and 2930 Ma for Ruossakero.

the other strongly negative (-354 ± 257). Also, one of the studied black schist samples shows a high γ Os value of +252, whereas two other samples have negative values of -943 and -437 at 2050 Ma (Fig. 9). The highly negative γ Os values could represent open-system behavior of sulfides and black schist samples, with Re having been gained in later orogeny-related processes. Trace sulfides in the co-magmatic Paleoproterozoic Jeesiörova komatiites also record highly negative γ Os values from -250 to -2370 (Gangopadhyay et al., 2006; Fig. 9), providing clear evidence for open-system behavior and gain of rhenium. The presence of minor radiogenic Os (at 2050 Ma, γ Os $+24 \pm 18$) in one mineralized chromite sample, which is located right above black schist in the drillcore (see Fig. 4 in Törmänen et al., 2016), is consistent with the previously measured heavy sulfur isotope compositions of sulfides; Törmänen et al. (2016) reported $\delta^{34}\text{S}$ values of $+9.8$ and $+15.5\text{\textperthousand}$ for two sulfide separates and $+11.3$ and $+15.0\text{\textperthousand}$ for two mineralized whole-rock samples. For country rock black schist samples, they obtained $\delta^{34}\text{S}$ values from $+17.2$ to $+24.4\text{\textperthousand}$, which are similar to the heavy sulfur isotope compositions measured by Grinenko et al. (2003) for sulfides from correlative black schists in the Kevitsa area ~ 23 km south of Lomalampi. Despite the sulfur isotope evidence for country rock interaction, the Os-rich chromites in the Lomalampi deposit have chondritic initial Os values, suggesting that the magma was not strongly contaminated by black schist material or that the contamination event postdated the time of chromite crystallization. Thus, both the sulfur and Os isotope data indicate a crustal isotope signature in the Lomalampi sulfides. One open question is the timing of the contamination process. One possibility is that radiogenic sulfides were formed at 1.85 Ga in a metamorphic event when ultramafic rocks and black schists interacted with metamorphic fluids, but a more realistic explanation is that magmatic sulfides were contaminated with Os from black schists when they formed at 2.05 Ga and later a metamorphic event reset their Os isotope system.

In summary, the close-to-chondritic initial osmium isotope ratios obtained for most chromites show that ore-forming processes are not

reflected in their Os isotope compositions. This may be a consequence of the contaminant being low in Os compared to the parental magma, but another option is that sulfide segregation took place late relative to chromite crystallization. To solve this problem, future studies should combine determinations of Os isotope composition of chromite with in-situ measurements of Ru in chromite (or other PGE), as it has been demonstrated recently by Locmelis et al. (2018) that the Ru contents of chromites are indicative of the presence or absence of a sulfide liquid during chromite crystallization.

5.3. The Re-Os ages and links to the regional geology

The new Re-Os isochron age of 2058 ± 93 Ma for the Paleoproterozoic Lomalampi PGE-(Ni-Cu) deposit links this deposit to the 2056 ± 25 Ma komatiitic magmatism of the Savukoski Group (Hanski et al., 2001b; Hanski and Huhma, 2005). This age group is important in terms of ore formation in the Central Lapland greenstone belt as it also includes the 2058 ± 4 Ma Kevitsa Ni-Cu-PGE deposit (Mutananen and Huhma, 2001).

The Tulppio Dunite has been interpreted to be Archean in age (DigiKp, 2018; Makkonen et al., 2017; Sorjonen-Ward and Luukkonen, 2005). Our new data, though somewhat ambiguous, are most consistent with a late Archean age for this ultramafic body. Our Re-Os date of 2719 ± 140 Ma obtained for the Vaara deposit correlates with the previous published U-Pb age of 2771 ± 8 Ma from a felsic enclave in an associated komatiitic rock (Papunen et al., 2009). According to our Re-Os age estimates, it seems that the Ruossakero deposit is older than the other studied Archean komatiite deposits. The Re-Os errorchron yields an age of 2990 ± 750 Ma, and the T_{RD} model age of one chromite separate with a near-chondritic γ Os value (-1.4) is 2942 ± 97 Ma. These are consistent with the U-Pb zircon age of 2.93 Ga (Karinen et al., 2015) from a felsic volcanic rock from the Ruossakero area. The bedrock in the Ruossakero area is regarded as being part of the Norrbotten tectonic province, whereas the other komatiitic deposits in Finland

occur in the Karelia tectonic province (Luukas et al., 2017). This may explain why the studied Ruossakero komatiites seem to be older than the other studied komatiites, with the age difference being ca. 100 Ma (ca. 2.93 Ga vs. 2.82 Ga). The > 2.90 Ga rocks in the Finnish part of the Karelia block are restricted to small occurrences of felsic volcanic rocks (ca. 2.93–2.94 Ga) in the Suomussalmi greenstone belt (Huhma et al., 2012a,b; Lehtonen et al., 2017). Instead, komatiites dated at ca. 2.9 Ga are abundant further to the east, in the Sumozero-Kenozero greenstone belt and Volotsk suite in the SE part of the Fennoscandian Shield in Russia (Puchtel et al., 1999, 2007).

6. Conclusions

The following conclusions can be drawn:

- (1) The Re-Os isochron age of 2058 ± 93 Ma for Paleoproterozoic Lomalampi PGE-(Ni-Cu) deposit correlates with the age of 2058 ± 4 Ma measured for the Kevitsa Ni-Cu-PGE deposit (Mutanen and Huhma, 2001) and the age of 2056 ± 25 Ma obtained for komatiites of the Savukoski Group in the Central Lapland greenstone belt (Hanski et al., 2001b). In terms of ore genesis, this ca. 2.05–2.06 Ga mafic-ultramafic magmatism (Hanski and Huhma, 2005) is an important stage in the evolution of the Central Lapland greenstone belt.
- (2) The new Re-Os age estimates of the Archean komatiitic deposits, Ruossakero (2990 ± 750 Ma), Vaara (2719 ± 140 Ma) and Tainiovaara (2753 ± 47 Ma), are in general agreement with the previous indirect age estimations for these deposits.
- (3) Most of the Os isotope compositions of the Os-rich (> 10 ppb) chromite separates from the studied Archean and Paleoproterozoic Ni-Cu deposits have near-chondritic initial γ Os values. This indicates that their Os is derived overwhelmingly from a mantle source with a chondritic Re-Os isotope evolution and in general, ore-forming processes are not reflected in the Os isotope signatures of chromites.
- (4) In the Paleoproterozoic Lomalampi PGE-(Ni-Cu) and Archean Tainiovaara Ni-(Cu-PGE) deposits, chromite separates from mineralized olivine cumulates yielded moderately high γ Os values ($+24 \pm 18$ and $+13 \pm 1$, respectively). This suggests some contamination with radiogenic Os. Its potential source is country rock black schist at Lomalampi, which is also supported by strong sulfur isotope evidence, but no Os-bearing sources are known in the neighborhood of the Tainiovaara deposit.
- (5) The Os isotope compositions of disseminated sulfides in the Vaara and Lomalampi deposits indicate resetting of the isotope system during a ca. 1.85 Ga metamorphic event. This together with isotope data from black schists shows that sulfides in both sedimentary and magmatic sulfide deposits were widely reset isotopically during the Svecofennian orogeny in eastern and northern Finland, both in the Archean basement and Paleoproterozoic supracrustal belts.

Acknowledgments

This work was supported by the Academy of Finland (grant 281859) and K.H. Renlund Foundation. We thank Riitta Kontio for assistance in mineral separation. Two anonymous reviewers are acknowledged for their constructive comments, which greatly helped to improve the manuscript. We are grateful to Franco Pirajno and Margaux LeVaillant for their editorial work.

References

- Amelin, Y., Li, C., Valeviev, O., Naldrett, A.J., 2000. Nd-Pb-Sr isotope systematics of crustal assimilation in the Voisey's Bay and Mushua intrusions, Labrador, Canada. *Econ. Geol.* 95, 815–830. <https://doi.org/10.2113/gsgeconeo.95.4.815>.
- Archer, G.J., Ash, R.D., Bullock, E.S., Walker, R.J., 2014. Highly siderophile elements and ^{187}Re - ^{187}Os isotopic systematics of the Allende meteorite: evidence for primary nebular processes and late-stage alteration. *Geochim. Cosmochim. Acta* 131, 402–414. <https://doi.org/10.1016/j.gca.2013.12.032>.
- Barnes, S.-J., Often, M., 1990. Ti-rich komatiites from northern Norway. *Contrib. Mineral. Petrol.* 105, 42–54. <https://doi.org/10.1007/BF00320965>.
- Bekker, A., Barley, M.E., Fiorentini, M.L., Rouxel, O.J., Rumble, D., Beresford, S.W., 2009. Atmospheric sulphur in Archaean komatiite-hosted nickel deposits. *Science* 326, 1086–1089. <https://doi.org/10.1126/science.1177742>.
- Brownscombe, W., Ihlendeld, C., Coppard, J., Hartshorne, C., Klatt, S., Siikalumoa, J.K., Herrington, R.J., 2015. The Sakatti Cu-Ni-PGE sulfide deposit in Northern Finland. In: Maier, W.D., Lahtinen, R., O'Brien, H. (Eds.), *Mineral Deposits of Finland*. Elsevier B.V., Amsterdam, pp. 211–252. <https://doi.org/10.1016/B978-0-12-410438-9.00009-1>.
- Condie, K.C., 2001. *Mantle Plumes and Their Record in Earth History*. Cambridge University Press, Cambridge. <https://doi.org/10.1017/CBO9780511810589>.
- Creaser, R.A., Papanastassiou, D.A., Wasserburg, G.J., 1991. Negative thermal ion mass-spectrometry of osmium, rhenium, and iridium. *Geochim. Cosmochim. Acta* 55, 397–401. [https://doi.org/10.1016/0016-7037\(91\)90427-7](https://doi.org/10.1016/0016-7037(91)90427-7).
- DigiKP, 2018. Bedrock of Finland 1:200 000 – Digital map database. Espoo, Geological Survey of Finland (accessed 21 August 2018) <https://hakku GTK.fi/en/locations/search>.
- Du, A.D., Zhao, D.M., Wang, S.X., Sun, D.Z., Liu, D.Y., 2001. Precise Re-Os dating for molybdenite by ID-NTIMS with Carius tube sample preparation. *Rock Miner. Anal.* 20, 247–252 (in Chinese with English abstract).
- Du, A.D., Wu, S.Q., Sun, D.Z., Wang, S.X., Qu, W.J., Markey, R., Stein, H., Morgan, J., Malinovskiy, D., 2004. Preparation and certification of Re-Os dating reference materials: molybdenites HLP and JDC. *Geostand. Geoanal. Res.* 28, 41–52. <https://doi.org/10.1111/j.1751-908X.2004.tb01042.x>.
- Du, A.D., Qu, W.J., Wang, D.H., Li, C., 2012. *Re-Os Dating and Its Application in Ore Deposits*. Geological Publishing House, Beijing (in Chinese).
- Fiorentini, M., Beresford, S., Barley, M., Duuring, P., Bekker, A., Rosengren, N., Cas, R., Hronsky, J., 2012. District to camp controls on the genesis of komatiite-hosted nickel sulfide deposits, Agnew-Wiluna greenstone belt, Western Australia: insights from the multiple sulfur isotopes. *Econ. Geol.* 107, 781–796. <https://doi.org/10.2113/econgeo.107.5.781>.
- Foster, J.G., Lambert, D.D., Frick, L.R., Maas, R., 1996. Re-Os isotopic evidence for genesis of Archean nickel ores from uncontaminated komatiites. *Nature* 382, 703–706. <https://doi.org/10.1038/382703a0>.
- Gangopadhyay, A., Walker, R.J., 2003. Re-Os systematics of the ca. 2.7-Ga komatiites from Alexo, Ontario, Canada. *Chem. Geol.* 196, 147–162. [https://doi.org/10.1016/S0009-2541\(02\)00411-4](https://doi.org/10.1016/S0009-2541(02)00411-4).
- Gangopadhyay, A., Walker, R.J., Hanski, E., Solheid, P.A., 2006. Origin of Paleoproterozoic komatiites at Jeesiöra, Kittilä greenstone complex, Finnish Lapland. *J. Petrol.* 47, 773–789. <https://doi.org/10.1093/petrology/egi093>.
- Grinenko, A.N., Hanski, E., Grinenko, V.A., 2003. Formation conditions of the Kevitsa Cu-Ni deposit: evidence from the S and C isotopes. *Geochem. Intern.* 41, 181–194.
- Gruau, G., Tourpin, S., Fourcade, S., Blais, S., 1992. Loss of isotopic (Nd, O) and chemical (REE) memory during metamorphism of komatiites: new evidence from eastern Finland. *Contrib. Mineral. Petrol.* 112, 66–82. <https://doi.org/10.1007/BF00310956>.
- Haapala, I., Papunen, H., 2015. A history of exploration for and discovery of Finland's ore deposits. In: Maier, W.D., Lahtinen, R., O'Brien, H. (Eds.), *Mineral Deposits of Finland*. Elsevier B.V., Amsterdam, pp. 1–38. <https://doi.org/10.1016/B978-0-12-410438-9.00001-7>.
- Halkoaho, T., Niskanen, M., 2004. A research report of nickel studies in the claim Jamali 1 area (claim register number 7626/1) in the Lieksa area during years 2002–2003. *Geol. Surv. Finl. Arch. Rep* M06/4314/2004/1/10.
- Hanski, E., 1980. Komatiitic and tholeiitic metavolcanics of the Siivilkovaara area in the Archean Kuhmo greenstone belt, eastern Finland. *Bull. Geol. Soc. Finl.* 52, 67–100. <https://doi.org/10.17741/bgsf/52.1.004>.
- Hanski, E., 2012. Evolution of the Palaeoproterozoic (2.50–1.95 Ga) non-orogenic magmatism in the eastern part of the Fennoscandian Shield. In: Melezhik, V.A., Prave, A.R., Hanski, E.J., Fallick, A.E., Lepland, A., Kump, L.R., Strauss, H. (Eds.), *Reading the Archive of Earth's Oxygenation. Volume 1, The Palaeoproterozoic of Fennoscandia as Context for the Fennoscandian Arctic Russia – Drilling Early Earth Project*. Springer, Berlin, Heidelberg, pp. 179–245. https://doi.org/10.1007/978-3-642-29682-6_6.
- Hanski, E.J., Huhma, H., 2005. Central Lapland greenstone belt. In: Lehtinen, M., Nurmi, P.A., Rämö, O.T. (Eds.), *Precambrian Geology of Finland – Key to the Evolution of the Fennoscandian Shield*. Elsevier B.V., Amsterdam, pp. 139–193. [https://doi.org/10.1016/S0166-2635\(05\)80005-2](https://doi.org/10.1016/S0166-2635(05)80005-2).
- Hanski, E.J., Kamenetsky, V.S., 2013. Chrome spinel-hosted melt inclusions in primitive Paleoproterozoic volcanic rocks, northern Finland: evidence for coexistence and mixing of komatiitic and picritic magmas. *Chem. Geol.* 343, 25–37. <https://doi.org/10.1016/j.chemgeo.2013.02.009>.
- Hanski, E.J., Huhma, H., Suominen, I.M., Walker, R.J., 1997. Geochemical and isotopic (Os, Nd) study of the early Proterozoic Keivitsa intrusion and its Cu-Ni deposit, northern Finland. In: Papunen, H. (Ed.), *Mineral Deposits: Research and Exploration – Where Do They Meet? Proceedings of the Fourth Biennial SGA Meeting*, Turku, 11–13 August, 1997. A. A. Balkema, Rotterdam, pp. 435–438.
- Hanski, E., Walker, R.J., Huhma, H., Suominen, I., 2001a. The Os and Nd isotopic systematics of the 2.44 Ga Akanvaara and Koitelainen mafic layered intrusions in northern Finland. *Precambr. Res.* 109, 73–102. [https://doi.org/10.1016/S0301-9268\(01\)00142-5](https://doi.org/10.1016/S0301-9268(01)00142-5).
- Hanski, E.J., Huhma, H., Rastas, P., Kamenetsky, V.S., 2001b. The Paleoproterozoic komatiite-picrite association of Finnish Lapland. *J. Petrol.* 42, 855–876. <https://doi.org/10.1093/petrology/42.5.855>.

- Hanski, E., Luo, Zh-Y., Odoro, H., Walker, R.J., 2011. The Pechenga Ni-Cu sulfide deposits, NW Russia: A review with new constraints from the feeder dikes. In: Li, C., Ripley, E.M. (Eds.), Magmatic Ni-Cu and PGE Deposits: Geology, Geochemistry, and Genesis. Rev. Econ. Geol. pp. 145–162.
- Hanski, E., Kontinen, A., Määttä, S., Lahtinen, H., Li, C., Qu, W.J., Yang, S.-H., 2016. Mo and Os as indicators of atmospheric oxygenation: evidence from Paleoproterozoic black shales at Talvivaara, eastern Finland. In: Abstracts of the 32nd Nordic Geological Winter Meeting, 13th to 15th of January, 2016, Helsinki, Finland, Bull. Geol. Soc. Finl. Spec. pp. 158–159.
- Heggie, G.J., Barnes, S.J., Fiorentini, M.L., 2013. Application of lithogeochemistry in the assessment of nickel-sulphide potential in komatiite belts from northern Finland and Norway. Bull. Geol. Soc. Finl. 85, 107–126.
- Heikura, P., Törmänen, T., Iljina, M., Salmirinne, H., 2010. Research report of Ni and PGE studies in the Tulppionkariste 1–5 claim areas, Savukoski commune (claim register numbers 8246/1–5). Geol. Surv. Finl., Rep M06/4723/2009/68. (in Finnish).
- Huhma, H., Määttä, I., Peltonen, P., Kontinen, A., Halkoaho, T., Hanski, E., Hokkanen, T., Hölttä, P., Juopperi, H., Konnunaho, J., Lahaye, Y., Luukkonen, E., Pietikäinen, K., Pulkkinen, A., Sorjonen-Ward, P., Vaasjoki, M., Whitehouse, M., 2012a. The age of the Archean greenstone belts in Finland. Geol. Surv. Finl., Spec. Pap. 54 In: Hölttä, P. (Ed.), The Archean of the Karelia Province in Finland, pp. 74–175.
- Huhma, H., Kontinen, A., Mikkola, P., Halkoaho, T., Hokkanen, T., Hölttä, P., Juopperi, H., Konnunaho, J., Luukkonen, E., Mutanen, T., Peltonen, P., Pietikäinen, K., Pulkkinen, A., 2012b. Nd isotopic evidence for Archean crustal growth in Finland. Geol. Surv. Finl., Spec. Pap. 54 In: Hölttä, P. (Ed.), The Archean of the Karelia Province in Finland, pp. 176–213.
- Juopperi, H., Vaasjoki, M., 2001. U-Pb mineral age determinations from Archean rocks in eastern Lapland. Geol. Surv. Finl., Spec. Pap. 33 In: Vaasjoki, M. (Ed.), Radiometric Age Determinations from Finnish Lapland and Their Bearing on the Timing of Precambrian Volcano-Sedimentary Sequences, pp. 209–227.
- Karinen, T., Lepistö, S., Konnunaho, J.P., Laura, S.L., Manninen, T., Huhma, H., 2015. Unit description report Enontekiö, Käsivarsi. Geol. Surv. Finl., Arch. Rep. 66/2015. (In Finnish).
- Keays, R.R., Lightfoot, P.C., 2010. Crustal sulfur is required to form magmatic Ni-Cu sulfide deposits: Evidence from chalcophile element signatures of Siberian and Deccan Trap basalts. Miner. Deposita 45, 241–257. <https://doi.org/10.1007/s00126-009-0271-1>.
- Konnunaho, J.P., 1999. Komatiites and their Ore Potential in the Archean Kovero greenstone belt. University of Oulu MSc thesis (in Finnish).
- Konnunaho, J.P., 2016. Komatiite-hosted Ni-Cu-PGE deposits in Finland: Their characterization, PGE contents, and petrogenesis. Academic Dissertation, Geological Survey of Finland, Espoo. <https://doi.org/10.13140/RG.2.1.1119.5929>.
- Konnunaho, J.P., Hanski, E.J., Bekker, A., Halkoaho, T.A.A., Hiebert, R.S., Wing, B.A., 2013. The Archean komatiite-hosted, PGE-bearing Ni-Cu sulphide deposit at Vaara, eastern Finland: evidence for assimilation of external sulphur and post-depositional desulphurization. Miner. Deposita 48, 967–989. <https://doi.org/10.1007/s00126-013-0469-0>.
- Konnunaho, J.P., Halkoaho, T.A.A., Hanski, E.J., Törmänen, T., 2015. Komatiite-hosted Ni-Cu-PGE deposits in Finland. In: Maier, W., O'Brian, H., Lahtinen, R. (Eds.), Mineral Deposits of Finland. Elsevier B.V., Amsterdam, pp. 93–128. <https://doi.org/10.1016/B978-0-12-410438-9.00004-2>.
- Lahaye, Y., Barnes, S.J., Frick, L.R., Lambert, D.D., 2001. Re-Os isotopic study of komatiitic volcanism and magmatic sulfide formation in the southern Abitibi greenstone belt, Ontario, Canada. Can. Mineral. 39, 473–490. <https://doi.org/10.2113/gscannmin.39.2.473>.
- Lahtinen, R., Korja, A., Nironen, M., 2005. Paleoproterozoic tectonic evolution. In: Lehtinen, M., Nurmi, P.A., Rämö, O.T. (Eds.), Precambrian Geology of Finland – Key to the Evolution of the Fennoscandian Shield. Elsevier B.V., Amsterdam, pp. 481–531. [https://doi.org/10.1016/S0166-2635\(05\)80012-X](https://doi.org/10.1016/S0166-2635(05)80012-X).
- Lambert, D.D., Foster, J.G., Frick, L.R., Ripley, E.M., Zientek, M.L., 1998. Geodynamics of magmatic Cu-Ni-PGE sulfide deposits: new in-sights from the Re-Os isotope system. Econ. Geol. 93, 121–136. <https://doi.org/10.2113/gsecongeo.93.2.121>.
- Lambert, D.D., Foster, J.G., Frick, L.R., Li, C., Naldrett, A.J., 1999. Re-Os isotopic systematics of the Voisey's Bay Ni-Cu-Co magmatic ore system, Labrador, Canada. Lithos 47, 69–88. [https://doi.org/10.1016/S0024-4937\(99\)00008-0](https://doi.org/10.1016/S0024-4937(99)00008-0).
- Lambert, D.D., Frick, L.R., Foster, J.G., Li, C., Naldrett, A.J., 2000. Re-Os isotopic systematics of the Voisey's Bay Ni-Cu-Co magmatic sulfide system. Canada: II. Implications for parental magma chemistry, ore genesis, and metal redistribution. Econ. Geol. 95, 867–888. <https://doi.org/10.2113/gsecongeo.95.4.867>.
- Lehtonen, E., Heilimo, E., Halkoaho, T., Käpyaho, A., Hölttä, P., 2016. U-Pb geochronology of Archean volcanic-sedimentary sequences in the Kuhmo greenstone belt, Karelia Province – multiphase volcanism from Meso- to Neoarchean and a Neoarchean depositional basin? Precambr. Res. 275, 48–69. <https://doi.org/10.1016/j.precamres.2015.12.002>.
- Lehtonen, E., Heilimo, E., Halkoaho, T., Hölttä, P., Huhma, H., 2017. The temporal variation of Mesoarchean volcanism in the Suomussalmi greenstone belt, Karelia Province, Eastern Finland. Int. J. Earth Sci. 106, 763–781. <https://doi.org/10.1007/s00531-016-1327-y>.
- Lehtonen, M., Airo, M.L., Eilu, P., Hanski, E., Kortelainen, V., Lanne, E., Manninen, T., Rastas, P., Räsänen, J., Virransalo, P., 1998. The stratigraphy, petrology and geochemistry of the Kittilä greenstone area, northern Finland: A report of the Lapland Volcanite Project. Geol. Surv. Finl., Rep. Invest. 140. (in Finnish with English summary).
- Lesher, C.M., Burnham, O.M., 2001. Multicomponent elemental and isotopic mixing in Ni-Cu-(PGE) ores at Kambalda, Western Australia, Canada. Can. Mineral. 39, 421–446. <https://doi.org/10.2113/gscannmin.39.2.421>.
- Lesher, C.M., Keays, R.R., 2002. Komatiite-associated Ni-Cu-(PGE) deposits: Geology, mineralogy, geochemistry and genesis. Can. Inst. Mining Metall., CIM Spec. In: Louis, J.C. (Ed.), The Geology, Geochemistry, Mineralogy and Mineral Beneficiation of Platinum-Group Elements, pp. 579–619.
- Lightfoot, P.C., Keays, R.R., 2005. Siderophile and chalcophile metal variations in flood basalts from the Siberian Trap, Noril'sk region: implications for the origin of the Ni-Cu-PGE sulfide ores. Econ. Geol. 100, 439–462. <https://doi.org/10.2113/gsecongeo.100.3.439>.
- Locmelis, M., Fiorentini, M.L., Barnes, S.J., Hanski, E., Kobussen, A.F., 2018. Ruthenium in chromite as an indicator for the magmatic sulfide ore potential of mafic-ultramafic systems. Ore Geol. Rev. 97, 152–170. <https://doi.org/10.1016/j.oregeorev.2018.05.002>.
- Ludwig, K.R., 2012. User's Manual for Isoplot 3.75 a Geochronological Toolkit for Microsoft Excel. Berkeley Geochronology Center Special Publication No. 5.
- Luolavirta, K., Hanski, E., Maier, W., Santaguida, F., 2017. Whole-rock and mineral compositional constraints on the magmatic evolution of the Ni-Cu-(PGE) sulfide ore-bearing Kevitsa intrusion, northern Finland. Lithos 296–299, 37–53. <https://doi.org/10.1016/j.lithos.2017.10.015>.
- Luukas, J., Kousa, J., Nironen, M., Vuollo, J., 2017. Major stratigraphic units in the bedrock of Finland, and an approach to tectonostratigraphic division. Metamorphism and Tectonic Evolution. Geol. Surv. Finl., Spec. Pap. 60 In: Nironen, M. (Ed.), Bedrock of Finland at the Scale 1:1 000 000 – Major Stratigraphic Units, pp. 9–39.
- Maier, W.D., Peltonen, P., Halkoaho, T., Hanski, E., 2013. Geochemistry of komatiites from the Tipasjärvi, Kuhmo, Suomussalmi, Ilomantsi and Tulppio greenstone belts, Finland: implications for tectonic setting and Ni sulphide prospectivity. Precambr. Res. 228, 63–84. <https://doi.org/10.1016/j.precamres.2012.12.004>.
- Makkonen, H.V., Halkoaho, T., Konnunaho, J., Rasilainen, K., Kontinen, A., Eilu, P., 2017. Ni-(Cu-PGE) deposits in Finland – geology and exploration potential. Ore Geol. Rev. 90, 667–696. <https://doi.org/10.1016/j.oregeorev.2017.06.008>.
- Mavrogenes, J.A., O'Neill, H.St.C., 1999. The relative effects of pressure, temperature and oxygen fugacity on the solubility of sulfide in mafic magmas. Geochim. Cosmochim. Acta 63, 1173–1180. [https://doi.org/10.1016/S0016-7037\(98\)00289-0](https://doi.org/10.1016/S0016-7037(98)00289-0).
- Metamorphism of Finland 1:1000 000. Digital map database. Espoo, Geological Survey of Finland (accessed 21 August 2018). <https://hakku GTK.fi/en/locations/search>.
- McDonough, W.F., Sun, S.-S., 1995. Composition of the Earth. Chem. Geol. 120, 223–253. [https://doi.org/10.1016/0009-2541\(94\)00140-4](https://doi.org/10.1016/0009-2541(94)00140-4).
- Mutanen, T., Huhma, H., 2001. U-Pb geochronology of the Koitelainen, Akanvaara and Keivitsa layered intrusions and related rocks. Geol. Surv. Finl., Spec. Pap. 33 In: Vaasjoki, M. (Ed.), Radiometric Age Determinations from Finnish Lapland and Their Bearing on the Timing of Precambrian Volcano-Sedimentary Sequences, pp. 229–246.
- Naldrett, A.J., 2004. In: Magmatic Sulfide Deposits Geology, Geochemistry and Exploration Springer. Berlin. <https://doi.org/10.1007/978-3-662-08444-1>.
- Nier, A.O., 1937. The isotopic constitution of osmium. Phys. Rev. 52, 885–892. <https://doi.org/10.1103/PhysRev.52.885>.
- Papunen, H., 1989. Platinium-group elements in metamorphosed Ni-Cu deposits in Finland. In: Prendergast, M.D., Jones, M.J. (Eds.), Magmatic Sulphides – the Zimbabwe Volume. The Institution of Mining and Metallurgy, London, pp. 165–176.
- Papunen, H., Halkoaho, T., Luukkonen, E., 2009. Archean evolution of the Tipasjärvi-Kuhmo Suomussalmi Greenstone Complex, Finland. In: Geol. Surv. Finl., Bull. pp. 403.
- Pekkarinen, L., 1980. The Tainiovaara Ni deposit in Lieksa. Geologi 7, 92 (in Finnish).
- Puchtel, I.S., Humayun, M., 2005. Highly siderophilic element geochemistry of ¹⁸⁷O-enriched 2.8-Ga Kostomuksha komatiites, Baltic Shield. Geochim. Cosmochim. Acta 69, 1607–1618. <https://doi.org/10.1016/j.gca.2004.09.007>.
- Puchtel, I.S., Arndt, N.T., Hofmann, A.W., Haase, K.M., Kröner, A., Kulikov, V.S., Kulikova, V.V., Garbe-Schönberg, C.-D., Nemchin, A.A., 1998a. Petrology of mafic lavas within the Onega plateau, central Karelia: evidence for 2.0 Ga plume-related continental crustal growth in the Baltic Shield. Contrib. Mineral. Petrol. 130, 134–153. <https://doi.org/10.1007/s004100050355>.
- Puchtel, I.S., Hofmann, A.W., Mezger, K., Jochum, K.P., Shchipansky, A.A., Samsonov, A.V., 1998b. Oceanic plateau model for continental crustal growth in the Archean: a case study from the Kostomuksha greenstone belt, NW Baltic Shield. Earth Planet. Sci. Lett. 155, 57–74. [https://doi.org/10.1016/S0012-821X\(97\)00202-1](https://doi.org/10.1016/S0012-821X(97)00202-1).
- Puchtel, I.S., Hofmann, A.W., Amelin, Y.V., Garbe-Schönberg, C.-D., Samsonov, A.V., Shchipansky, A.A., 1999. Combined mantle plume-island arc model for the formation of the 2.9 Ga Sumozero Kenozero greenstone belt, SE Baltic Shield: isotope and trace element constraints. Geochim. Cosmochim. Acta 63, 3579–3595. [https://doi.org/10.1016/S0016-7037\(99\)00111-8](https://doi.org/10.1016/S0016-7037(99)00111-8).
- Puchtel, I.S., Brügmann, G.E., Hofmann, A.W., Kulikov, V.S., Kulikova, V.V., 2001. Os isotope systematics of komatiitic basalts from the Vetreny belt, Baltic Shield: evidence for a chondritic source of the 2.45 Ga plume. Contrib. Mineral. Petrol. 140, 588–599. <https://doi.org/10.1007/s00410000203>.
- Puchtel, I.S., Brandon, A.D., Humayun, M., Walker, R.J., 2005. Evidence for the early differentiation of the core from Pt-Re-Os isotope systematics of 2.8-Ga komatiites. Earth Planet. Sci. Lett. 237, 118–134. <https://doi.org/10.1016/j.epsl.2005.04.023>.
- Puchtel, I.S., Humayun, M., Walker, R.J., 2007. Os-Pb-Nd isotope and highly siderophilic and lithophile trace element systematics of komatiitic rocks from the Volotsk suite, SE Baltic Shield. Precambr. Res. 158, 119–137. <https://doi.org/10.1016/j.precamres.2007.04.004>.
- Räsänen, J., Hanski, E., Lehtonen, M., 1989. Komatiites, low-Ti tholeites and andesites in the Möykkelä area. In: Central Finnish Lapland. Geol. Surv. Finl., Rep. Invest. pp. 88.
- Ripley, E.M., Li, C., 2013. Sulfide saturation in mafic magmas: is external sulfur required for magmatic Ni-Cu-(PGE) ore genesis? Econ. Geol. 108, 45–58. <https://doi.org/10.2113/econgeo.108.1.45>.
- Seat, Z., Beresford, S.W., Grguric, B.A., Gee, M.A.M., Grassineau, N.V., 2009. Reevaluation of the role of external sulfur addition in the genesis of Ni-Cu-PGE

- deposits: evidence from the Nebo-Babel Ni-Cu-PGE deposit, West Musgrave, Western Australia. Econ. Geol. 104, 521–538. <https://doi.org/10.2113/gsecongeo.104.4.521>.
- Shirey, S.B., Walker, R.J., 1998. Re-Os isotopes in cosmochemistry and high temperature geochemistry. Ann. Rev. Earth Planet. Sci. 26, 423–500. <https://doi.org/10.1146/annurev.earth.26.1.423>.
- Smoliar, M.I., Walker, R.J., Morgan, J.W., 1996. Re-Os ages of group IIA, IIIA, IVA and VIB iron meteorites. Science 271, 1099–1102.
- Smythe, D.J., Wood, B.J., Kiseeva, E.S., 2017. The S content of silicate melts at sulfide saturation: new experiments and a model incorporating the effects of sulfide composition. Am. Mineral. 102, 795–803. <https://doi.org/10.2138/am-2017-5800CCBY>.
- Sorjonen-Ward, P., Luukkonen, E.J., 2005. Archean rocks. In: Lehtinen, M., Nurmi, P.A., Rämö, O.T. (Eds.), Precambrian Geology of Finland – Key to the Evolution of the Fennoscandian Shield. Elsevier B.V., Amsterdam, pp. 19–99. [https://doi.org/10.1016/S0166-2635\(05\)80003-9](https://doi.org/10.1016/S0166-2635(05)80003-9).
- Staude, S., Barnes, S.J., Vaillant, M.L., 2016. Evidence of lateral thermomechanical erosion of basalt by Fe-Ni-Cu sulfide melt at Kambalda, Western Australia. Geology 44, 1047–1050. <https://doi.org/10.1130/G37977.1>.
- Staude, S., Barnes, S.J., Vaillant, M.L., 2017. Thermomechanical erosion of ore-hosting embayments beneath komatiite lava channels: textural evidence from Kambalda, Western Australia. Ore Geol. Rev. 90, 446–464. <https://doi.org/10.1016/j.oregeorev.2017.05.001>.
- Törmänen, T., Konnunaho, J.P., Hanski, E., Moilanen, M., Heikura, P., 2016. The Paleoproterozoic komatiite-hosted PGE mineralization at Lomalampi, Central Lapland Greenstone Belt, northern Finland. Miner. Deposita 51, 411–430. <https://doi.org/10.1007/s00126-015-0615-y>.
- Vanne, J., 1981. A Research report of nickel studies concerning the claim of Tainiovaara 1 (register number of claim 2538/1). Geol. Surv. Finl., Arch. Rep. M. 06/4332/81/1/10. (in Finnish).
- Walker, R.J., Morgan, J.W., Horan, M.F., Czamanske, G.K., Krogstad, E.J., Fedorenko, V.A., Kunilov, V.E., 1994. Re-Os isotopic evidence for an enriched-mantle source for the Noril'sk-type, ore-bearing intrusions, Siberia. Geochim. Cosmochim. Acta 58, 4179–4197. [https://doi.org/10.1016/0016-7037\(94\)90272-0](https://doi.org/10.1016/0016-7037(94)90272-0).
- Walker, R.J., Morgan, J.W., Hanski, E.J., Smolkin, V.F., 1997. Re-Os systematics of early Proterozoic ferropicrites, Pechenga Complex, Russia: evidence for ancient ¹⁸⁷Os enriched plumes. Geochim. Cosmochim. Acta 61, 3145–3160. [https://doi.org/10.1016/S0016-7037\(97\)00088-4](https://doi.org/10.1016/S0016-7037(97)00088-4).
- Yang, S.-H., Hanski, E., Li, C., Maier, W.D., Huhma, H., Mokrushin, A.V., Latypov, R., Lahaye, Y., O'Brien, H., Qu, W.-J., 2016. Mantle source of the 2.44–2.50-Ga mantle plume-related magmatism in the Fennoscandian Shield: evidence from Os, Nd, and Sr isotope compositions of the Monchel pluton and Kemi intrusions. Miner. Deposita 51, 1055–1073. <https://doi.org/10.1007/s00126-016-0673-9>.